

Accepted Manuscript

Systematic screening and characterization of Qi-Li-Qiang-Xin capsule-related xenobiotics in rats by ultra-performance liquid chromatography coupled with quadrupole time-of-flight tandem mass spectrometry

Wei-jing Yun, Zhi-hong Yao, Cai-lian Fan, Zi-fei Qin, Xi-yang Tang, Meng-xue Gao, Yi Dai, Xin-sheng Yao



PII: S1570-0232(18)30193-4

DOI: [doi:10.1016/j.jchromb.2018.05.014](https://doi.org/10.1016/j.jchromb.2018.05.014)

Reference: CHROMB 21178

To appear in:

Received date: 1 February 2018

Revised date: 29 April 2018

Accepted date: 10 May 2018

Please cite this article as: Wei-jing Yun, Zhi-hong Yao, Cai-lian Fan, Zi-fei Qin, Xi-yang Tang, Meng-xue Gao, Yi Dai, Xin-sheng Yao , Systematic screening and characterization of Qi-Li-Qiang-Xin capsule-related xenobiotics in rats by ultra-performance liquid chromatography coupled with quadrupole time-of-flight tandem mass spectrometry. The address for the corresponding author was captured as affiliation for all authors. Please check if appropriate. Chromb(2017), doi:[10.1016/j.jchromb.2018.05.014](https://doi.org/10.1016/j.jchromb.2018.05.014)

This is a PDF file of an unedited manuscript that has been accepted for publication. As a service to our customers we are providing this early version of the manuscript. The manuscript will undergo copyediting, typesetting, and review of the resulting proof before it is published in its final form. Please note that during the production process errors may be discovered which could affect the content, and all legal disclaimers that apply to the journal pertain.

Systematic screening and characterization of Qi-Li-Qiang-Xin capsule-related xenobiotics in rats by ultra-performance liquid chromatography coupled with quadrupole time-of-flight tandem mass spectrometry

Wei-jing Yun ^a, Zhi-hong Yao ^b, Cai-lian Fan ^a, Zi-fei Qin ^b, Xi-yang Tang ^b, Meng-xue Gao ^b, Yi Dai ^{b,*}, Xin-sheng Yao ^{a,b,*}

^a College of Traditional Chinese Materia Medica, Shenyang Pharmaceutical University, Shenyang 110016, P.R. China;

^b College of Pharmacy and Guangdong Provincial Key Laboratory of Pharmacodynamic Constituents of TCM and New Drugs Research, Jinan University, Guangzhou 510632, P.R. China

* Corresponding authors:

Prof. Xin-sheng Yao, College of Traditional Chinese Materia Medica, Shenyang Pharmaceutical University, 110016, P.R. China; Tel: +86 24 23993994; Fax: +86 24 23993994; E-mail: tyaoxs@gmail.com;

Prof. Yi Dai, College of Pharmacy, Jinan University, Guangzhou 510632, P.R. China; Tel: +86 20 85220785; Fax: +86 20 85221559; E-mail: daiyi1004@163.com

Abstract:

Qi-Li-Qiang-Xin capsule (QLQX), a well-known traditional Chinese medicine prescription (TCMP), consisted of eleven commonly used herbal medicines, has been widely used for the treatment of chronic heart failure (CHF). However, the absorbed components and related metabolites after oral administration of QLQX are still remaining unknown. In the present work, a reliable and effective method using ultra performance liquid chromatography coupled with quadrupole time-of-flight tandem mass spectrometry (UPLC/Q-TOF-MS) was established to identify QLQX-related xenobiotics in rats. Based on a representative structure based homologous xenobiotics identification (RSBHXI) strategy, a total of eleven compounds (salvianolic acid B, formononetin, benzoylmesaconine, alisol A, sinapine thiocyanate, naringin, tanshinone IIA, ginsenoside Rg1, ginsenoside Rb1, astragaloside IV and periplocin), bearing different chemical core structures, were selected and investigated for their metabolism *in vivo*. And then, comprehensive metabolic profiles of the holistic multi-ingredients in QLQX were achieved. As a result, a total of 121 QLQX-related xenobiotics (47 prototypes and 74 metabolites) were identified or tentatively characterized, among them eight prototypes (mesaconine, hypaconine, songorine, fuziline, neoline, talatizamine formononetin, neocryptotanshinone) and two metabolites (calycosin-gluA, formononetin-guaA) were relatively the main existing xenobiotics exposed in blood. All absorbed prototype constituents were mainly from six composed herbal medicines (Aconiti lateralidis radix, Astragali radix, Ginseng radix, Alismatis rhizoma, Salvia miltiorrhiza radix, Periploca cortex). The main metabolic

reactions were methylation, hydrogenation, hydroxylation, oxidization, sulfation and glucuronidation. This is the first study on *in vivo* metabolism of QLQX. These results enabled us to focus on several high exposure ingredients in the discovery of effective substances of QLQX, however further pharmacokinetic study on these QLQX-related xenobiotics are needed to be carried out.

Keywords: Qi-Li-Qiang-Xin capsule; chemical profile; representative compounds; metabolites profiles; metabolic pathways; UPLC/Q-TOF-MS;

1. Introduction

Qi-Li-Qiang-Xin capsule (QLQX), a traditional Chinese medicine prescription, consisted of eleven commonly used herbal medicines, including Astragali radix, Ginseng radix, Aconiti lateralis radix, Salvia miltiorrhiza radix, Semen descurainiae lepidii, Alismatis rhizoma, Polygonati odorati rhizoma, Cinnamomi ramulus, Carthami flos, Periploca cortex and Citri reticulatae pericarpium [1]. It has been widely used for treatment of chronic heart failure (CHF), and its safety and efficacy had been re-confirmed by a multicenter, randomized, double-blind, parallel-group, placebo-controlled clinical trials [2]. Recent pharmacological studies showed that QLQX possessed various activities, including improving cardiac function [3], attenuating cardiac remodeling [4], protecting cardiac myocytes and mitochondrial function [5].

However, the effective constituents of QLQX are still remaining unknown. Few reports were available on the *in vivo* metabolism of QLQX. The metabolic fates of some component herbal medicines of QLQX had been reported, such as Astragali

radix [6], Ginseng radix [7], Aconiti lateralis radix [8], Salvia miltorrhiza radix [9], the metabolic profiles of holistic QLQX could not be deduced due to the inevitable drug-drug-interactions between the component herbal medicines. Therefore, comprehensive studies on the holistic metabolic profiles of multiple ingredients in QLQX *in vivo* are important and indispensable. In our previous study, a “representative structure based homologous xenobiotics identification” (RSBHXI) strategy was proposed and had been successfully applied for rapid identification of the xenobiotics of a six-herbal-medicines-composed TCM prescription XLGB capsule in rats after oral administration [10]. In this study, rapid identification of chemical ingredients in QLQX was performed with the help of an in-house database, which included all compounds isolated and identified from each composed herbal medicines of QLQX reported in literatures, as well as comparison of reference standards. And then, prototypes were screened out in a preliminary experiment, with the same UPLC/Q-TOF-MS condition established in chemical recognition of QLQX. Eleven representative compounds, bearing different core structures, were selected among the observed prototypes for investigation of their metabolic fates *in vivo*, individually. All information of identified metabolites of each representative compound was collected (including retention time and MS fragmentation patterns) and added into the in-house database, which was used for screening out potential metabolites of QLQX. All QLQX-related xenobiotics were further affirmed by comparison of their retention time and main MS fragment ions with the updated database. In addition, metabolic reactions and diagnostic ions, found in single compounds related metabolites, were

also employed as supplementary approaches to discover more homologous metabolites.

2. Experimental

2.1. Materials and reagents

QLQX powder and the plant materials (Astragali radix, Ginseng radix, Aconiti lateralis radix, Salvia miltiorrhiza radix, Semen descurainiae lepidii, Alismatis rhizoma, Polygonati odorati rhizoma, Cinnamomi ramulus, Carthami flos, Periploca cortex and Citri reticulatae pericarpium) were provided by Shijiazhuang Yiling Pharmaceutical Co., Ltd. (Hebei, China). Salvianolic acid B, salvianolic acid A, formononetin, benzoylmesaconine, alisol A, calycosin-7-*O*-β-D-glucopyranoside, calycosin, sodium danshensu, hesperidin, ginsenoside Rb₂, ginsenoside Rc, 20(S)-ginsenoside Rg₂, 20(S)-ginsenoside F₂, cinnamaldehyde, chlorogenic acid and sinapine thiocyanate were purchased from Shanghai Ronghe Medical Technological Co., Ltd. (Shanghai, China). Tanshinone IIA, cryptotanshione, rosmarinic acid, alisol F, alisol B, alisol B 23-acetate, songorine, neoline, fuziline, mesaconitine, talatizamine, hypaconitine, rutin, naringin, nobiletin, ginsenoside Rg₁, ginsenoside Rb₁, ginsenoside Re, ginsenoside Rd, astragalosides I, astragalosides II, astragaloside IV and periplocin were purchased from Chengdu Chroma-Biotechnology CO., LTD. (Chengdu, China). Quercetin-3-*O*-β-D-glucopyranosyl-7-*O*-β-gentioside, kaempferol-3-*O*-β-D-glucopyranosyl-7-*O*-β-gentioside, isorhamnetin-3,7-di-*O*-β-D-glucopyranosyl, isorhamnetin-3-*O*-β-D-glucopyranoside and quercetin-3-*O*-β-D-glucopyranoside were isolated from Semen descurainiae

lepidii in the authors' laboratory and their structures were confirmed by NMR and MS spectral method. The purity of each compound was more than 98% determined by HPLC analysis. LC–MS grade acetonitrile and water were purchased from Fisher Scientific (Fair Lawn, New Jersey, USA). LC–MS grade formic acid was obtained from Sigma-Aldrich (St. Louis, USA). Water, methanol and ethanol were all of HPLC grade.

2.2. Sample preparation

QLQX powder (1 g) was suspended in 10 mL methanol in an ultrasonic water bath for 30 min at room temperature. 2.0 μ L supernatant aliquot was injected for analysis after centrifugation at 14,000 rpm for 10 min.

For drug administration, QLQX powder was suspended in water then orally administered to rats at 2 g/kg/d. Periplocin, alisol A and sinapine thiocyanate were suspended in 0.5% CMC-Na solution and were given to rats at gavage of 40 mg/kg, respectively. Tanshinone IIA, ginsenoside Rg1, ginsenoside Rb1, astragaloside IV, salvianolic acid B, formononetin and naringin were also suspended in 0.5% CMC-Na solution and were ingested to rats at 100 mg/kg, respectively. As an exception, benzoylmesaconine was given to rats at 10 mg/kg by oral gavage. The rats (n=3) in QLQX group and rats (n=3) in each single component group were oral administration for three days, and blood samples were collected on Day 3. Rats (n=3) in blank group were ingested by water, and blood samples collection method was the same as QLQX group.

2.3. Animals and drug administration

Male Sprague-Dawley rats (220-250) g were obtained from the experimental animal center of Guangdong province (Guangzhou, China). They were housed at ambient temperature of (20 ± 2) °C with 12-h light/dark cycles for two weeks before experiment and fed a standard diet and water ad libitum. Water was free access to animals in metabolic cages separately over night before experiment. The animal protocols were approved by the Guide for the Care and Use of Laboratory Animals of Jinan University. All procedures were in accordance with Guide for the Care and Use of Laboratory Animals (National Institutes of Health).

2.4. Biological samples collection and pretreatment

Biological samples including plasma, urine and feces were collected as follows:

Plasma samples: The rats were anesthetized by intraperitoneal injection of 10% aqueous chloral hydrate. The blood samples were collected from hepatic portal vein in heparinized tube at three different time points (0.5 h, 1 h and 2 h), and centrifuged at 12,000 rpm for 10 min, respectively. The serum samples were mixed, and an aliquot of 2 mL was treated with 6 mL acetonitrile to precipitated protein. After centrifuging at 12,000 rpm for 10 min, the supernatant was dried under nitrogen gas at room temperature. The residue was dissolved in 300 μL methanol.

Urine samples: Urine samples were collected for 0-24 h. The urine sample (2 mL) was loaded on a HLB column (6 m³, 200 mg, Waters Oasis, Ireland) directly, and then eluted by 6 mL of 5% methanol and 6 ml of methanol successively. The methanol eluate was collected and dried under nitrogen gas at room temperature. The residue was reconstituted in 300 μL methanol.

Feces samples: Feces samples were collected for 0–24 h. Feces were dried in air and then crushed into crude powder. The powder (1.0 g) was extracted by 10-fold of methanol in an ultrasonic bath for 30 min. After centrifuging at 12,000 rpm for 10 min, the supernatant was dried under reduced pressure. The residue was reconstituted in 300 µL methanol.

2.5. UPLC-Q/TOF-MS analysis

UPLC analysis was carried out on an ACQUITYTM UPLC I-Class system comprised a quaternary pump, a diode-array detector (DAD), an autosampler, and a column compartment. Samples were separated on an Acquity UPLC BEH C₁₈ Column (2.1 mm × 100 mm, 1.7 µm) at a temperature of 40 °C. The mobile phases consisted of eluent A (0.1% formic acid in water, v/v) and eluent B (0.1% formic acid in acetonitrile, v/v) using a gradient program as follow: 2% B from 0 to 1 min, 2–70% B from 1 to 18 min, 70–100% B from 18 to 20 min. After holding 100% B for next 2 min, the column was returned to its starting condition. The flow rate was kept at a 0.4 mL/min and the injection volume was 2 µL for all the samples.

UPLC system was coupled to a quadrupole time-of-flight tandem mass spectrometry (SYNAPTTM G2 HDMS, Waters, Manchester, U.K.) equipped with electrospray ionization (ESI). The operating parameters were set as follow: Capillary voltage of 3 kV (ESI+) or -2.5 kV (ESI-); Sample cone voltage of 35 V; Extraction cone voltage of 4 V, source temperature of 100 °C, desolvation temperature 400 °C, cone gas flow of 50 L/h and desolvation gas flow of 800 L/h. In MS^E mode, trap collision energy was 4 eV for low energy function and 20–50eV for high energy

function. Argon was used as collision gas for CID in both MS^E and MS^2 mode. The mass spectrometer was calibrated over a range of 50-2000 Da using solution of sodium formate. Leucine-enkephalin (m/z 556.2771 in positive ion mode; m/z 554.2615 in negative ion mode) was used as external reference of LockSprayTM infused at a constant flow of 5 μ L/min. Argon was used as collision gas. All data were processed with software UNIFI 1.7.0 (waters, Manchester, U.K.) and Masslynx V4.1 (waters, Manchester, U.K.).

3. Results and discussion

3.1. Characterization of chemical constituents in QLQX.

The base peak ion chromatograms (BPIs) of QLQX by UPLC/Q-TOF-MS in positive and negative ion modes were presented in Fig. 1. A total of 173 compounds were identified and tentatively characterized, including 34 flavanoids, 33 alkaloids, 44 saponins, 31 triterpenes, 4 cardiac glycosides, 7 phenolic acids, 5 tanshinones, 4 hydroxycinnamic acid derivatives, 1 sesquiterpenes, 1 diterpene, 4 oligosaccharides and 5 phenylpropanoids (Table S1). Among them, 44 compounds were unambiguously identified by comparison with reference standards. Other compounds were tentatively characterized based on accurate mass of quasimolecular, fragmentation pathways and MS spectra with the literature. The mass error for molecular ions of all compounds identified in this study was within ± 5 ppm.

3.2. Characterization of metabolites of eleven representative single compounds in rat

Eleven compounds were selected, covered 8 component herbal medicines, including astragaloside IV, formononetin, ginsenoside Rg1, ginsenoside Rb1,

tanshinone IIA, salvianolic acid B, periplocin, benzoylmesaconine, alisol A, sinapine thiocyanate and naringin. The eleven compounds contain a variety of chemical structure types (shown in Fig. 2) and have a relatively high content in QLQX (Fig. 1). Besides, all of them have correlative bioactivities, such as cardioprotective effects [11], anti-myocardial ischemia [12] and cardiotonic action [13]. The related metabolites of each representative compound in rat urine, plasma and feces samples were detected on the platform of Metabolynx XS software under the manipulation system of Masslynx (V4.1, Waters Corporation, Milford, MA). And then, their structures were further characterized by MS fragmentation patterns.

3.3.1. Metabolites identification of formononetin

After oral administration of formononetin (**1**), 15 related metabolites were identified in plasma, urine and feces samples. Metabolite **5** was observed at the retention time of 7.74 min and yielded a protonated molecule $[M+H]^+$ ion at m/z 255.0651. Its molecular formula was established as $C_{15}H_{10}O_4$, indicating it was demethylated derivative of **1**. Metabolites **3** and **4** showed precursor ion at m/z 335.0215, 80 Da higher than **1**. The neutral loss of the sulfate group made the fragment ion at m/z 255.0649, and the characteristic fragment ions at m/z 227.0704, 199.0758, 181.0685 were observed. Thus, metabolites **3** and **4** were proposed to be sulfated formononetin.

Metabolites **6** ($t_R = 8.30$ min), **8** ($t_R = 8.58$ min) and **10** ($t_R = 9.53$ min) were isomers with the same protonated ion at m/z 285.0758 ($C_{16}H_{12}O_5$), 16 Da heavier than parent compound. Mass fragment ions at m/z 270.0510 $[M+H-CH_3\cdot]^+$ and 253.0492

$[M+H-CH_3OH]^+$ were both found in the MS/MS spectra of these metabolites. Interestingly, metabolite **6** had a characteristic fragment ion at m/z 137.023 $[^{1,3}A+H]^+$, whereas metabolites **8** and **10** yielded m/z 152.0120 $[^{1,3}A+H]^+$, indicating that hydroxylation was occurred at the different sites of formononetin (**1**). Taking the retention time into account, metabolites **6** ($CLogP = 1.91$), **8** ($CLogP = 2.16$) and **10** ($CLogP = 2.98$) were identified as the hydroxylated products.

Besides, formononetin (**1**) could be biotransformed to metabolites **12** and **16**, and then underwent dehydration, hydroxylation and glucuronidation reaction to produce a series of metabolites (**11**, **14** and **15**). Additionally, formononetin (**1**) also could be metabolized to metabolite **13** by hydrogenation [14, 15]. Taken altogether, proposed metabolic pathways of chemical structures and metabolic transformations were shown in Fig. S1.

3.3.2 Metabolites identification of astragaloside IV

A total of 12 metabolites (Table 1) were identified from biological sample after oral administration of astragaloside IV (17), according to MS fragmentation patterns of saponins in Astragali radix and their metabolites reported in literatures [16,17]. Metabolites **27**, **28** and **29** showed $[M+Na]^+$ ions at m/z 675.4064, 645.3947, and 513.5349, respectively. They were formed by loss of glucose and arabinose from prototype. On the basis of diagnostic ions at m/z 473.3634 $[aglycone+H-H_2O]^+$, 455.3514 $[aglycone+H-2H_2O]^+$, 437.3405 $[aglycone+H-3H_2O]^+$, 419.3290 $[aglycone+H-4H_2O]^+$, these metabolites were characterized as dexylcosylation products of astragaloside IV. In addition, metabolite **24** was identified as a

dehydrogenation metabolite of astragaloside IV, since its mother and daughter ions (Table 1) were all 2 Da less than that of the parent drug (astragaloside IV). Similarly, Metabolite **25** showed same fragment ions but 18 Da less than **17**, which was assigned as a dehydration product of astragaloside IV.

Metabolites **18-20**, **22** and **23** exhibited a $[M+H]^+$ at m/z 947.5219 ($C_{47}H_{78}O_{19}$), 162 Da more than astragaloside IV. The information of further MS/MS fragment ions at m/z 473.3648, 455.3553, 437.3402, 419.3300 indicated that they were biotransformation components of astragaloside IV after glycosylation. Metabolites **21** and **26**, with the same characteristic ions, were tentatively identified as shown in Fig. S2.

3.3.3. Metabolites identification of ginsenoside Rg1

As a result, 24 related metabolites were identified in plasma, urine and feces samples, after oral administration of ginsenoside Rg1 (**30**). Two possible oxidation metabolites of Rg1 (metabolites **32** and **33**) were detected, assigned reasonably as mono-oxidation metabolites of Rg1. Both of them exhibited $[M+Na]^+$ ions at m/z 839.4763, which molecular weight were 16 Da greater than that of ginsenoside Rg1. The deglycosylated product ions could be observed in the MS/MS spectra of metabolites **32** and **33**, including the $[M+H\text{-glc}\text{-H}_2O]^+$, $[M+H\text{-glc}\text{-2H}_2O]^+$ and $[M+H\text{-2glc}\text{-3H}_2O]^+$ ions at m/z 637.4312, 619.4211 and 439.3546, respectively. Metabolite **35** exhibited an $[M+Na]^+$ ion at m/z 855.4738, 32 Da greater than ginsenoside Rg1. Its MS/MS fragmentation patterns were quite analogous with oxidation metabolites (**32** and **33**). Therefore, metabolite **35** was identified as

di-oxidation metabolites. Metabolites **31**, **34** and **36-38** were formed by hydrogenation, dehydrogenation and hydrolysis after oxidation. Metabolites **47** and **48** showed $[M+Na]^+$ ions at m/z 865.4923 ($C_{44}H_{74}O_{15}$), 42 Da more than ginsenoside Rg1. They all yielded a major product ion at m/z 801.4631, generated by loss of C_2H_2O moiety. This information indicated that metabolites 47 and 48 were the acetylation products of ginsenoside Rg1.

Metabolites **49** and **50** showed $[M+Na]^+$ ions at m/z 661.4369, 162 Da less than ginsenoside Rg1, which was consistent with a glucose. Hence, they were classified into deglycosylated metabolites of ginsenoside Rg1. Ginsenoside Rg1 could be transformed into metabolite **54** by the loss of two glucose groups. A series of dehydrated product ions in MS/MS information (Table 1) gave further approve [18].

Metabolites **39**, **41**, **43** and **45** were isomers with the same molecular formula of $C_{48}H_{82}O_{19}$ (m/z 963.5558), 162 Da more than ginsenoside Rg1. In their MS/MS spectra, the characteristic ion at m/z 783.4941 formed by loss of glucose group indicated that the glycosylation was occurred. Detailed information about them was listed in Table 1. Speculated chemical structures were shown in Fig. S3.

3.3.4. Metabolites identification of ginsenoside Rb1

After oral administration of ginsenoside Rb1 (**55**), a total of 15 metabolites were identified from biosample (Table 1). Deglycosylation and oxidation were the most major metabolic pathways of ginsenoside Rb1. Metabolite **56** showed $[M+Na]^+$ at m/z 1147.5961 ($C_{54}H_{92}O_{24}$), 16 Da more than **55**, indicating introduction of an O into the molecule of Rb1. The MS/MS spectra of metabolite **56** showed fragment ions

corresponding to the sequential loss of glucose moieties (Figure S4; Table 1). Metabolites **58**, **59**, **64-68** and **70** were identified to be deglycosylated products of Rb1. Notably, metabolites (**60-63** and **69**) derived from de-glycosylation and subsequent oxidation were also observed. Besides, metabolite **57** was a glycosylated product of Rb1. These metabolites were confirmed according to precursor, molecular formula and characteristic fragment ions as listed in (Table 1). According to the literatures [19-21], the possible metabolic pathways of ginsenoside Rb1 were presumed in Fig. S4.

3.3.5. Metabolites identification of salvianolic acid B

Finally, 12 related metabolites (Table 1) were identified in feces samples, after oral administration of salvianolic acid B (**71**). These metabolites could be grouped as methylated and hydrolysed metabolites according to the mass data. Metabolites **72-76** were formed by ester bond hydrolysis. Metabolite **76** gave an $[M-H]^-$ signal at m/z 537.1047 ($C_{27}H_{22}O_{12}$), 180 Da less than salvianolic acid B, indicating that it was generated by lose of $C_9H_8O_4$ moiety. Metabolite **76** was designated to be lithospermic acid A, by comparing the mass spectra with literature [22]. Metabolites **74** and **75** displayed the same $[M-H]^-$ ion at m/z 539.1185, were the hydrolysis products since salvianolic acid B had the two ester bonds which could undergo hydrolysis reaction at two sites. Metabolite **73** was assigned as salvianolic acid R, which originated from the hydrolysis of all the two ester bonds and furan ring in salvianolic acid B. In addition, the cleavages of two ester bonds in metabolite **73** would lead to form Metabolite **72** [22, 23]. As shown in Fig. S5, seven methylated products of salvianolic acid B were

elucidated by analysis of the MS spectra. Metabolites **77-79** showed the $[M-H]^-$ ion at m/z 731.1596, 14 Da heavier than that of salvianolic acid B, suggesting that they might be methylated salvianolic acid B. The characteristic fragment ions at m/z 533.1078, 353.0604, 339.0509, 335.0555, 321.0399, corresponding to $[M-H-C_9H_{10}O_5]^-$, $[M-H-C_9H_{10}O_5-C_9H_8O_4]^-$, $[M-H-C_9H_{10}O_5-C_{10}H_{10}O_4]^-$, $[M-H-C_9H_{10}O_5-C_9H_8O_4-H_2O]^-$ and $[M-H-C_{10}H_{12}O_5-C_9H_8O_4-H_2O]^-$, were used for characterization. Metabolites **80-83** were identified as methylated salvianolic acid B, due to the similar fragmentations with above metabolites [22, 23]. Proposed chemical structures and metabolic transformations of the metabolites were presented in Fig. S5.

3.3.6. Metabolites identification of tanshinone IIA

A total of 17 metabolites (Table 1) were identified from the rat plasma, urine and feces samples after oral administration of tanshinone IIA (**84**). According to the published works, hydroxylation was the major metabolic transformations of tanshinone IIA [24-26]. Its monohydroxylated (**89, 93, 95.**) and dihydroxylated (**86-88, 92**) metabolites were identified in this paper. Metabolite **96** displayed $[M+Na]^+$ at m/z 335.1248, 2 Da more than hydroxyl tanshinone IIA. Metabolite **97** showed $[M+Na]^+$ at m/z 337.1405, 4 Da more than monohydroxyl tanshinone IIA. Hence, they were identified as hydrogenated products of monohydroxyl tanshinone IIA. Metabolites **85, 90, 91** and **94** were isomers with the same $[M+Na]^+$ ions at m/z 351.1199. The MS/MS characteristic ions of them were m/z 311.1253 $[M+H-H_2O]^+$, 267.1381 $[M+H-C_2O]^+$, 225.0908 $[M+H-C_2O-C_3H_6]^+$ (Fig. S1). These characteristic fragment ions were 2 Da more than those in dihydroxyl tanshinone IIA, suggesting that they

were hydrogenated metabolites of dihydroxyl tanshinone IIA. Metabolites **98-101** were produced by the reaction of hydroxylation, methylation or dehydrogenation from tanshinone IIA. Detailed information about the metabolites was listed in Table 1, and proposed chemical structures and metabolic transformations were shown in Fig. S6.

3.3.7. Metabolites identification of benzoylmesaconine

In consideration of the poisonousness about benzoylmesaconine (**102**) and relative high ionization efficiency in electrospray MS, the oral dose of benzoylmesaconine in rats (10 mg/kg/d) was chose less than that of the other single compounds. A total of 17 metabolites (Table 1) were identified from the rat plasma, urine and feces samples, and proposed chemical structures and metabolic transformations were shown in Fig. S7.

Metabolites **103** and **104** were identified as mesaconine and hypaconine compared with reference standards. Metabolites **107-109** exhibited a pseudo-molecule ion $[M+H]^+$ at m/z 606.2927 ($C_{31}H_{43}NO_{11}$), 16 Da higher than **102**. The MS/MS spectrum showed fragment ions at m/z 588.2809, 574.2679, 556.2513, 524.2244. According to the literature, they were identified as hydroxyl-benzoylmesaconine [27]. Metabolites **105**, **106**, **112** and **115** showed pseudo-molecule ion $[M+H]^+$ at m/z 576.2786 ($C_{30}H_{41}NO_{10}$), which lacked a CH_2 group from the parent compound. The major fragmentations at m/z 558.2648, 526.2432, 512.2304, 494.2162, all of them were 14 Da lower than the fragment ions from parent molecule. Therefore, they were identified as demethylated metabolites of benzoylmesaconine. Metabolites **111** and **118** were estimated to be methyl-benzoylmesaconine according to the fragment ions

which were 14 Da higher than parent molecule. Metabolites **111** and **118** could be biotransformed to metabolites **110** and **119** through metabolic reaction of dehydrogenation and hydroxylation. Metabolite **113** showed $[M+H]^+$ at *m/z* 588.2814, which confirmed the smart molecular formula ($C_{31}H_{41}NO_{10}$), had a loss of 2 Da from parent molecule, indicating that it was dehydrogenated metabolites of benzoylmesaconine. Metabolites **114**, **116** and **117** gave the quasi-molecular ions of $[M+H]^+$ at *m/z* 574.3013 ($C_{31}H_{43}NO_9$), 16 Da less than benzoylmesaconine. The MS/MS spectrum of them showed fragmentation ions at *m/z* 556.2959 $[M+H-H_2O]^+$, 542.2712 $[M+H-H_2O-CH_2]^+$, 524.2652 $[M+H-2H_2O-CH_2]^+$, 510.2460 $[M+H-2H_2O-2CH_2]^+$, which were also 16 Da lower than the corresponding fragments generated by benzoylmesaconine. Hence, they were identified as shown in table 1.

3.3.8. Metabolites identification of periplocin

As shown in Table 1, 14 metabolites were identified from plasma, urine and feces samples after oral administration of periplocin (**120**). *In vivo*, periplocin could be metabolized into metabolites **128** (periplogenin) and **133** (periplocyarin) by deglycosylation [28], and then underwent demethylation, hydroxylation and hydroxylation reaction to produce a series of metabolites. The molecular formula of metabolites **122** and **125** were determined to be $C_{23}H_{34}O_6$ ($[M+H]^+ m/z$ 407.2432), 16 Da heavier than periplogenin (**128**). In the MS/MS spectra, they showed the fragment ions at *m/z* 389.2326 $[M+H-H_2O]^+$, 371.2223 $[M+H-2H_2O]^+$, 353.2114 $[M+H-3H_2O]^+$, 335.2009 $[M+H-4H_2O]^+$. Therefore, metabolites **122** and **125** were determined as hydroxylated metabolites of **128**. Metabolites **121**, **123** and **126**

exhibited the same $[M+Na]^+$ at m/z 431.2401, and their molecular formulas were established as $C_{23}H_{36}O_6$, which were 18 Da higher than that of **128**. In their MS/MS spectra, fragment ion at m/z 391.2475 was also 18 Da heavier than that in **128**.

Metabolite **130** exhibited a protonated ion at m/z 537.3422, and the molecular formula was $C_{30}H_{48}O_8$, similar with that of **134**. The MS/MS spectrum of them showed fragment ions at m/z 375.2528 $[M+H-glc]^+$, 357.2428 $[M+H-glc-H_2O]^+$, 339.2316 $[M+H-glc-2H_2O]^+$, which were 2 Da more than that of **133**. So, they were determined as hydrogenated products of periplocyarin. Metabolite **131** gave an $[M+H]^+$ signal at m/z 521.3124 ($C_{29}H_{44}O_8$), 14 Da less than that of **133**. The MS/MS spectrum of **131** showed a fragment ion at m/z 391.2470 formed by lose of $C_6H_{10}O_3$ moiety, indicated that the demethylation was occurred on the glycosyl moiety. Proposed chemical structures and metabolic transformations of the metabolites were presented in Fig. S8.

3.3.9. Metabolites identification of alisol A

A total of 20 metabolites (Table 1) were identified in plasma, urine and feces samples after oral administration of alisol A (**135**). The protonated ion of metabolite **146** was at m/z 507.3667 ($C_{30}H_{50}O_6$), 16 Da more than the parent compound. The MS/MS spectrum fragment ions at m/z 489.3580, 471.3498, 453.3358, 381.2779, 363.2683, indicated that it was hydroxylated product of alisol A [29]. Metabolite **155** showed $[M+Na]^+$ at m/z 511.3399 ($C_{30}H_{48}O_6$) which had 2 Da (H_2) less than alisol A [29]. The diagnostic fragment ions at m/z 471.3456, 453.3301, 381.2784 and 337.2509, were also 2 Da less than that in alisol A. Therefore, **155** was deduced as

dehydrogenated metabolite of alisol A. Metabolites **137** and **138** exhibited the same $[M+H]^+$ at m/z 491.3375, their molecular formulas were established as $C_{29}H_{46}O_6$. Based on the fragment ions at m/z 473.3276 $[M+H-H_2O]^+$, 455.3172 $[M+H-2H_2O]^+$, 437.3047 $[M+H-3H_2O]^+$, 419.2917 $[M+H-4H_2O]^+$, 401.2694 $[M+H-C_4H_{10}O_2]^+$, they were determined as hydroxylation product of demethylated alisol A.

Metabolites **151** and **153** exhibited the same $[M+Na]^+$ at m/z 689.3865, with the molecular formula of $C_{36}H_{58}O_{11}$. In their MS/MS spectra, fragmentations at m/z 473.3606 was generated by lose of glucuronic acid and H_2O . Accordingly, they were tentatively identified as glucuronide conjugate of alisol A. Besides, phase I metabolites (**139-144**, **148**, **149**), phase II metabolites (**147**, **150**, **154**) were tentatively identified. The proposed chemical structures of all metabolites were tentatively identified as shown in Fig. S9.

3.3.10. Metabolites identification of sinapine thiocyanate

After oral administration of sinapine thiocyanate (**156**), a total of 4 metabolites (Table 1) were identified from the rat urine and feces samples. *In vivo*, parent compound could be biotransformed to metabolite **160** by lose of $C_4H_{10}N^+$ moiety. Metabolites **158** and **159** exhibited the same $[M+H]^+$ at m/z 225.0776, generated by lose of $C_5H_{12}N^+$ moiety. Different fragment ions at m/z 167.0709 and 181.0876, showed in their MS/MS spectrometry, indicated that they underwent demethylation reaction at different sites of the structure. The proposed chemical structures as shown in Fig. S10. At last, metabolites **158** underwent hydrogenation reaction to produce metabolites **157**.

3.3.11. Metabolites identification of naringin

According to the MS information and their metabolites reported in literatures [30, 31], 15 related metabolites (Table 1) were identified in plasma, urine and feces samples, after oral administration of naringin (**161**). Metabolite **166** showed $[M-H]^-$ ion at m/z 609.1824 ($C_{28}H_{34}O_{15}$), 30 Da (CH_2+O) heavier than parent compound. In the MS/MS spectra, characteristic ions at m/z 301.0717 $[M-H-C_{12}H_{20}O_9]^-$, 271.0658 $[M-H-C_{12}H_{20}O_9-CH_2O]^-$, 151.0043 $[^{1,3}A^-]$ were used for characterization of flavonoids. According to the literature [30], metabolite **166** was identified as hesperidin. Additionally, metabolite **166** also could be metabolized to metabolites **172** and **176** by deglycosylation and sulfation. Metabolite **169** was confirmed as hydrogenated naringin for the $[M-H]^-$ ion at m/z 581.188 ($C_{27}H_{34}O_{14}$), 2 Da (H_2) more than naringin, and the fragment ions at m/z 273.0763, 179.0344 and 119.0507 [30].

In vivo, naringin could be metabolized to naringenin (**162**) by deglycosylation reaction, and a series of metabolites (**163**, **164**, **166**, **168-171** and **173-175**) were produced through reaction of dehydrogenation, hydrogenation, sulfation and glucuronidation [30, 31]. All proposed chemical structures as shown in Fig. S11.

3.4. Characterization of absorbed QLQX constituents and related metabolites

To systematically elucidate the absorbed constituents and metabolites of QLQX *in vivo*, a dosage of QLQX (2 g/kg) was oral administration to rats. As a result, a total of 121 xenobiotics were identified or tentatively characterized in plasma, urine and feces samples. Among them, 65 xenobiotics in QLQX had been also detected (Table 1) in eleven representative single compounds related metabolites. Beyond that,

according to the MS fragmentations and metabolic pathways of representative compounds, another 56 QLQX-related xenobiotics (29 prototypes and 27 metabolites) were identified as shown in Table 2. EICs of major QLQX-related xenobiotics in biological samples were shown in Fig. 3.

The main metabolic pathways for aconitum alkaloids were dehydrogenation, methylation, demethylation, hydroxylation and dehydration as described in 3.3.7. According to that, other metabolites derived from aconitum alkaloids were screened out. Metabolite **177** showed a protonated molecular ion $[M+H]^+$ at *m/z* 424.2692 ($C_{23}H_{37}NO_6$), 16 Da heavier than isotalatizidine. It was diagnosed as hydroxylation product of isotalatizidine by analyzing characteristic fragmentations *m/z* 406.2590 $[M+H-H_2O]^+$, which was also 16 Da heavier than that of isotalatizidine. Metabolite **179** showed $[M+H]^+$ at *m/z* 360.2533 ($C_{22}H_{33}NO_3$), 2 Da less than **178**, and the characteristic fragment ion at *m/z* 342.2344, generated by lose of H_2O , indicated that it was hydrogenated songorine. Metabolites **180**, **183** and **185** were identified as methylation of aconitum alkaloids, according to their fragmentations formed by lose of CO, H_2O and CH_3OH . Phase II metabolites (**192-194**) of isoflavone were detected in rat biological samples, and presented in relatively high abundance. They were identified by the characteristic fragmentation with the neutral loss of 80 or 176 Da in MS/MS spectra. Metabolites **199** and **221** had the similar characteristic ions and metabolic pathways with diterpene quinones, were identified as shown in Table 2. Metabolites **212** and **213** exhibited the same $[M+Na]^+$ at *m/z* 323.1258 ($C_{18}H_{20}O_4$), 14 Da (CH_2) less than neocryptotanshinone (**224**). The MS/ MS spectrum of them

showed fragmentation ions at m/z 283.1335 $[M+H-H_2O]^+$, 265.1230 $[M+H-2H_2O]^+$, 255.1381 $[M+H-H_2O-CO]^+$. Thus, they were tentatively identified as demethylation of neocryptotanshinone. Hydroxylation was the most common metabolic pathway with alisol A, other alisols were the same. Metabolite **214** showed $[M+H]^+$ at m/z 505.3529 ($C_{30}H_{48}O_6$), 16 Da more than the parent compound. The MS/MS spectrum fragment ions at m/z 487.3346, 469.3365, corresponding to $[M+H-H_2O]^+$, $[M+H-2H_2O]^+$, were assisted for identification. Then it was tentatively identified as hydroxylated product of alisol F. Metabolites **217**, **223** and **225-227** were all hydroxylation products of alisols, identified them with information as shown in Table 2.

The chemical compositions of QLQX included flavonoids, saponins, cardiac glycosides, diterpene quinones, phenolic acids, diterpene alkaloids and triterpenoids. Hydroxylation, methylation, demethylation, sulfation and glucuronidation were familiar metabolic pathways of flavonoids. As for saponins, the major metabolic reaction was hydrolysis. In the case of diterpene quinones, reduction, hydroxylation, and methylation were main metabolic pathways. Meanwhile, the most important metabolic reaction of phenolic acids was ester hydrolysis. There were many metabolic pathways for aconitum alkaloids such as dehydrogenation methylation, demethylation, hydroxylation and dehydration. Obviously, the triterpenoids mainly undertook hydroxylation and demethylation.

In addition, twelve prototypes [mesaconine (**2**), hypaconine (**7**), songorine (**178**), fuziline (**182**), neoline (**184**), talatizamine (**187**), formononetin (**110**), ginsenoside Rg1

(**63**), Ginsenoside Rb1 (**105**), alisol A (**169**), periplogenin (**83**), neocryptotanshinone (**224**) and two metabolites [calycosin-gluA (**192**), formononetin-gluA (**194**)] were the main xenobiotics exposed in rat's plasma after oral administration of QLQX at 2g/kg/d. By far as we known, mesaconine (**2**) and hypaconine (**7**) possessed cardiotonic activities [32], talatizamine (**187**) showed cardio-protective effect *in vitro* [33], while songorine (**178**) had antiarrhythmic, antinociceptive and anti-inflammatory properties [34]. The two very important isoflavonoids from Astragali radix, calycosin and formononetin, were known well due to their antioxidant properties as well as the treatment for cardiovascular disease [35]. Research had demonstrated that ginsenoside Rb1 could decrease cardiac contraction at the ventricular myocyte level [36]. Alisol A, as one of major active component from Alismatis rhizoma, exerted considerable diuretic effects [37]. Periplogenin (**83**) was found in rat plasma which is a representative constituent derived from Periploca cortex. According to the report [38], periplogenin (**83**) played a protective role in cardiovascular problems. Therefore, these main xenobiotics with reported *in vitro* bioactivities and clinical application were considered to play key roles in therapeutic effects of QLQX.

All absorbed prototype components were mainly originated from Aconiti lateralis radix, Astragali radix, Ginseng radix, Alismatis rhizoma, Salvia miltiorrhiza radix and Periploca cortex. It put forward a demand that more chemical markers from these herbal medicines should be monitored, when developing quality control methods for chemical consistency evaluation between multiple batches of QLQX.

4. Conclusion

A total of 173 compounds, including triterpenes, saponins, alkaloids, flavanoids, phenolic acids, cardiac glycosides, tanshinones, hydroxycinnamic acid derivatives and oligosaccharides, were identified or tentatively characterized in QLQX by UPLC/Q-TOF-MS. Among them, eleven representative compounds, bearing different core structures, were selected as parent drug for further investigation on their metabolic profiles in rats after orally administrated, individually. Totally, 176 metabolites were screened out and then characterized in rat's plasma, urine and feces. Based on retention times and MS characteristic fragmentation patterns of ingredients detected in QLQX and the metabolites of eleven compounds, a total of 121 QLQX-related xenobiotics were identified or tentatively characterized, including 38 in plasma, 82 in urine, 47 in feces. The main metabolic reactions involved methylation, hydrogenation, hydroxylation, oxidization, sulfation and glucuronidation. This is the first study on *in vivo* metabolism of QLQX. It revealed some main exposed xenobiotics (e.g. the twelve prototypes and two metabolites) for the further pharmacological and pharmacokinetic study of QLQX.

Acknowledgments

We are grateful to Shijiazhuang Yiling Pharmaceutical Co., Ltd. for providing the Qi-Li-Qiang-Xin capsule. This work was supported by the National Major Scientific and Program of Introducing Talents of Discipline to Universities (B13038).

Declaration of interest

All the authors report no declarations of interest.

References

- [1] Chinese Pharmacopoeia Commission, Pharmacopoeia of the People Republic of China, Chinese Medical Science and Technology Press, Beijing 2015, 1, 922-923.
- [2] X. L. Li, J Zhang, J. Huang, A. Ma, J. F. Yang, W. M. Li, Z. G. Wu, C. Yao, Y. H. Zhng, W. M. Yao, B. Zhang, R. L. Gao. A multicenter, randomized, double-blind, parallel-group, placebo-controlled study of the effects of qili qiangxin capsules in patients with chronic heart failure. *J. Am. Coll. Cardiol.* 62 (2013) 1065-1072.
- [3] X. Hong, Y. Song, Y. Li, Y. H. Liao, J. Chen. Qiliqiangxin regulates the balance between tumor necrosis factor- α and interleukin-10 and improves cardiac function in rats with myocardial infarction. *Cell Immunol.* 260 (2009) 51-55.
- [4] L. C. Tao, S. T. Shen, S. Y. Fu, H. Y. Fang, X. Z. Wang, S. Das, J. P. G. Sluijter, A. Rosenzweig, Y. L. Zhou, X. Q. Kong, J. J. Xiao, X. L. Li. Traditional Chinese Medication Qiliqiangxin attenuates cardiac remodeling after acute myocardial infarction in mice. *Sci. Rep.* 5 (2015) 1-10.
- [5] J. M. Zhou, K. Jiang, X. F. Ding, M. Q. Fu, S. J. Wang, L. T. Zhu, T. He, J. F. Wang, A. J. Sun, K. Hu, L. Chen, Y. Z. Zou, J. B. Ge. Qiliqiangxin inhibits angiotensin II-induced transdifferentiation of rat cardiac fibroblasts through suppressing interleukin-6. *J. Cell Mol. Med.* 19 (2015) 1114-1121.
- [6] Z. Y. Zhang, B. Wu, Y. H. Tang, Z. X. Li, Z. L. Sun, L. Y. Chen, Y. B. Ji, C. H. Ma, C. G. Huang. Characterization of major flavonoids, triterpenoid, dipeptide and their metabolites in rat urine after oral administration of Radix Astragali decoction. *J. Anal.*

Chem. 68 (2013) 716-721.

[7] J. R. Wang, L. F. Yau, T. T. Tong, Q. T. Feng, L. P. Bai, J. Ma, M. Hu, L. Li, Z. H.

Jiang. Characterization of oxygenated metabolites of ginsenoside Rb1 in plasma and urine of rat. *J. Agric. Food. Chem.* 63 (2015) 2689-2700.

[8] G. G. Tan, Z. Y. Lou, J. Jing, W. H. Li, Z. Y. Zhu, L. Zhao, G. Q. Zhang, Y. F. Chai.

Screening and analysis of aconitum alkaloids and their metabolites in rat urine after oral administration of aconite roots extract using LC-TOF-MS-based metabolomics.

Biomed. Chromatogr. 25 (2011) 1343-1351.

[9] X. Zhao, D. H. Yang, F. Xu, S. Huang, L. Zhang, G. X. Liu, S. Q. Cai. The in vivo

absorbed constituents and metabolites of Danshen decoction in rats identified by

HPLC with electrospray ionization tandem ion trap and time-of-flight mass spectrometry. *Biomed. Chromatogr.* 29 (2015) 285-304.

[10] J. L. Geng, Y. Dai, Z. H. Yao, Z. F. Qin, X. L. Wang, L. Qin, X. S. Yao.

Metabolites profile of Xian-Ling-Gu-Bao capsule, a traditional Chinese medicine prescription, in rats by ultra performance liquid chromatography coupled with quadrupole time-of-flight tandem mass spectrometry analysis. *J. Pharm. Biomed. Anal.* 96 (2014) 90-103.

[11] X. Yan, J. X. Liu, H. J. Wu, Y. Liu, S. D. Zheng, C. Y. Zhang, C. Yang. Impact of

miR-208 and its Target Gene Nemo-Like Kinase on the Protective Effect of Ginsenoside Rb1 in Hypoxia/Ischemia Injured Cardiomyocytes. *Cell Physiol. Biochem.* 39 (2016) 1187-1195.

[12] C. Y. Su, Q. L. Ming, K. Rahman, T. Han, L. P. Qin. *Salvia miltiorrhiza*:

traditional medicinal uses, chemistry, and pharmacology. *Chin. J. Nat. Med.* 13 (2015) 163-182.

[13] X. F. Chen, Y. Cao, H. Zhang, Z. Y. Zhu, M. Liu, H. B. Liu, X. Ding, Z. Y. Hong, W. H. Li, D. Y. Lv, L. R. Wang, X. Y. Zhou, J. P. Zhang, X. Q. Xie, Y. F. Chai.

Comparative normal/failing rat myocardium cell membrane chromatographic analysis system for screening specific components that counteract doxorubicin-induced heart failure from Aconitum carmichaeli. *Anal. Chem.* 86 (2014) 4748-4757.

[14] S. M. Heinonen, K. Wähälä, H. Adlercreutz. Identification of urinary metabolites of the red clover isoflavones formononetin and biochanin A in human subjects. *J. Agric. Food Chem.* 52 (2004) 6802-6809.

[15] M. H. Liu, P. L. Li, X. Zeng, H. X. Wu, W. W. Su, J. Y. He. Identification and pharmacokinetics of multiple potential bioactive constituents after oral administration of radix astragali on cyclophosphamide-induced immunosuppression in Balb/c mice. *Int. J. Mol. Sci.* 16 (2015) 5047-5071.

[16] X. D. Cheng, M. G. Wei. Profiling the metabolism of astragaloside IV by ultra performance liquid chromatography coupled with quadrupole/time-of-flight mass spectrometry. *Molecules*, 19 (2014) 18881-18896.

[17] R. N. Zhou, Y. L. Song, J. Q. Ruan, Y. T. Wang, R. Yan. Pharmacokinetic evidence on the contribution of intestinal bacterial conversion to beneficial effects of astragaloside IV, a marker compound of astragali radix, in traditional oral use of the herb. *Drug Metab. Pharmacokinet.* 27 (2012) 586-597.

[18] X. Y. Wang, C. C. Wang, F. F. Pu, P. Y. Lin, T. X. Qian. Metabolite profiling of

ginsenoside Rg1 after oral administration in rat. *Biomed Chromatogr.* 28 (2014) 1320-1324.

[19] T. X. Qian, Z. H. Jiang, Z. C. Cai. High-performance liquid chromatography coupled with tandem mass spectrometry applied for metabolic study of ginsenoside Rb1 on rat. *Anal. Biochem.* 352 (2006) 87-96.

[20] G. G. Chen, M. Yang, Y. Song, Z. Q. Lu, J. Q. Zhang, H. L. Huang, S. H. Guan, L. J. Wu, D. A. Guo. Comparative analysis on microbial and rat metabolism of ginsenoside Rb1 by high-performance liquid chromatography coupled with tandem mass spectrometry. *Biomed Chromatogr.* 22 (2008) 779-785.

[21] J. R. Wang, L. F. Yau, T. T. Tong, Q. T. Feng, L. P. Bai, J. Ma, M. Hu, L. Liu, Z. H. Jiang. Characterization of oxygenated metabolites of ginsenoside Rb1 in plasma and urine of rat. *J. Agric. Food Chem.* 63 (2015) 2689-2700.

[22] Q. Qu, H. Kun, F. Y. Li, L. J. Cao, G. J. Wang, H. P. Hao. The identification and pharmacokinetic studies of metabolites of salvianolic acid B after intravenous administration in rats. *Chin. J. Nat. Med.* 11 (2013) 560-565.

[23] M. Xu, H. Guo, J. Han, S. F. Sun, A. H. Liu, B. R. Wang, D. A. Guo. Structural characterization of metabolites of salvianolic acid B from *Salvia miltiorrhiza* in normal and antibiotic-treated rats by liquid chromatography–mass spectrometry. *J. Chromatogr. B.* 858 (2007) 184-198.

[24] P. Li, G. J. Wang, J. Li, H. P. Hao, C. N. Zheng. Characterization of metabolites of tanshinone IIA in rats by liquid chromatography/tandem mass spectrometry. *J. Mass Spectrom.* 41 (2006) 670-684.

- [25] J. H. Sun, M. Yang, X. M. Wang, M. Xu, A. H. Liu, D. A. Guo. Identification of tanshinones and their metabolites in rat bile after oral administration of TTE-50, a standardized extract of *Salvia miltiorrhiza* by HPLC-ESI-DAD-MSⁿ. *J. Pharm. Biomed. Anal.* 44 (2007) 564-574.
- [26] Y. J. Wei, P. Li, C. G. Wang, Y. R. Peng, L. Shu, X. B. Jia, B. Wang. Metabolism of tanshinone IIA, cryptotanshinone and tanshinone I from *Radix Salvia Miltorrhiza* in zebrafish. *Molecules*, 17 (2012) 8617-8632.
- [27] L. Ye, X. S. Yang, L. L. Lu, W. Y. Chen, S. Zeng, T. M. Yan, L. N. Dong, X. J. Peng, J. Shi, Z. Q. Liu. Monoester-diterpene aconitum alkaloid metabolism in human liver microsomes: predominant role of CYP3A4 and CYP3A5. *Evid. Based Complement Alternat Med.* 2013 (2012) 1-24.
- [28] J. He, F. Bo, Y. Tu, J. T. Azietaku, T. Dou, H. Z. Ouyang, X. M. Gao. A validated LC-MS/MS assay for the simultaneous determination of periplocin and its two metabolites, periplocyarin and periplogenin in rat plasma: Application to a pharmacokinetic study. *J. Pharm. Biomed. Anal.* 114 (2015) 292-295.
- [29] Y. Yu, Z. Z. Liu, P. Ju, Y. Y. Zhang, L. H. Zhang, K. S. Bi, X. H. Chen. *In vitro* metabolism of alisol A and its metabolites' identification using high-performance liquid chromatography-mass spectrometry. *J. Chromatogr. B.* 941 (2013) 31-37.
- [30] M. H. Liu, W. Zou, C. P. Yang, W. Peng, W. W. Su. Metabolism and excretion studies of oral administered naringin, a putative antitussive, in rats and dogs. *Biopharm Drug Dispos.* 33 (2012) 123-134.
- Pereira-Caro, G., Ludwig, I. A., Polyviou, T., Malkova, D., García, A., Moreno-Rojas,

- [31] G. P. Caro, I. A. Ludwig, T. Polyviou, D. Malkova, A. Garcia, J. M. Morenorojas, A. Crozier. Identification of Plasma and Urinary Metabolites and Catabolites Derived from Orange Juice (Poly) phenols: Analysis by High-Performance Liquid Chromatography–High-Resolution Mass Spectrometry. *J. Agric. Food Chem.* 64 (2016) 5724-5735.
- [32] X. X. Jian, P. Tang, X. X. Liu, R. B. Chao, Q. H. Chen, X. K. She, F. P. Wang. Structure-cardiac activity relationship of C19-diterpenoid alkaloids. *Nat. Prod. Commun.* 7 (2012) 713-720.
- [33] X. F. Chen, Y. Cao, H. Zhang, Z. Y. Zhu, M. Liu, H. B. Liu, X. Ding, Z. Y. Hong, W. H. Li, D. Y. Lv, L. R. Wang, X. Y. Zhou, J. P. Zhang, X. Q. Xie, Y. F. Chai. Comparative normal/failing rat myocardium cell membrane chromatographic analysis system for screening specific components that counteract doxorubicin-induced heart failure from Aconitum carmichaeli. *Anal. Chem.* 86 (2014) 4748-4757.
- [34] H. Khan, S. M. Nabavi, A. Sureda, N. Mehterov, D. Gulei, I. Berindan-Neagoe, A. G. Atanasov. Therapeutic potential of songorine, a diterpenoid alkaloid of the genus Aconitum. *Eur. J. Med. Chem.* 11 (2017) 1-5.
- [35] X. Huang, Y. Liu, F. G. Song, Z. Q. Liu, S. Y. Liu. Studies on principal components and antioxidant activity of different Radix Astragali samples using high-performance liquid chromatography/electrospray ionization multiple-stage tandem mass spectrometry. *Talanta*, 78 (2009) 1090-1101.
- [36] G. I. Scott, P. B. Colligan, B. H. Ren, J. Ren. Ginsenosides Rb1 and Re decrease cardiac contraction in adult rat ventricular myocytes: role of nitric oxide. *Br. J.*

Pharmacol. 134 (2001) 1159-1165.

[37] X. Zhang, X. Y. Li, N. Lin, W. L. Zhao, X. Q. Huang, Y. Chen, M. Q. Huang, X. Wen, S. S Wu. Diuretic activity of compatible triterpene components of Alismatis rhizoma. Molecules, 22 (2017) 1459.

[38] S. Panda, A. Kar. Periplogenin, isolated from *Lagenaria siceraria*, ameliorates L-T4-induced hyperthyroidism and associated cardiovascular problems. Horm. Metab. Res. 43 (2011) 188-193.

Table List

Table 1 Characterization of *in vivo* metabolites of eleven representative single compounds of QLQX in rats.

Table 2 Characterization of *in vivo* metabolites of QLQX in rats (metabolites characterized in Table 1 are not included).

Table 1 Characterization of *in vivo* metabolites of eleven representative single compounds of QLQX in rats.

	<i>t</i> _R /min	selected ion	elemental composition	Measured mass	ppm	fragmentation	Identification	Source (single comp.)	Source (formula)
1	10.44	[M+H] ⁺	C ₁₆ H ₁₂ O ₄	269.0807	-2.6	253.0493,237.0543,197.0604	Formononetin	P.U.F	P.U.F
2	5.68	[M+H] ⁺	C ₁₅ H ₁₀ O ₈ S	351.016	-4.3	271.0596,255.0678	Formononetin-CH ₂ +O+sul	U	
3	5.75	[M+H] ⁺	C ₁₅ H ₁₀ O ₇ S	335.0215	-3.0	255.0649,227.0704,199.0758,181.0685	Formononetin-CH ₂ +sul	U	
4	6.38	[M+H] ⁺	C ₁₅ H ₁₀ O ₇ S	335.0235	3.0	255.0649,227.0704,199.0758,181.0685	Formononetin-CH ₂ +sul isomer	P	P
5	7.74	[M+H] ⁺	C ₁₅ H ₁₀ O ₄	255.0651	-2.4	227.0704,199.0758,181.0685	Formononetin-CH ₂	P.U.F	
6	8.30	[M+H] ⁺	C ₁₆ H ₁₂ O ₅	285.0758	-1.8	270.0510,253.0492,225.0542,137.0233	Calcosin	U	U
7	8.42	[M+H] ⁺	C ₂₂ H ₂₀ O ₁₁	461.1117	7.2	285.0756,270.0510	Formononetin+gluA+O	P	U
8	8.58	[M+H] ⁺	C ₁₆ H ₁₂ O ₅	285.0759	-1.4	270.0510,253.0492,229.0860,152.0120	Formononetin+O	U	
9	8.94	[M+H] ⁺	C ₁₆ H ₁₂ O ₇ S	349.0369	-3.7	269.0804,253.0493,237.0543,197.0604	Formononetin+sul	U	
10	9.53	[M+H] ⁺	C ₁₆ H ₁₂ O ₅	285.0753	-0.7	270.0510,253.0492,229.0860,152.0120	Formononetin+O	U.F	U
11	9.67	[M+Na] ⁺	C ₂₁ H ₂₂ O ₉	441.1179	4.1	283.0958,255.0646	Formononetin-CH ₂ +H ₂ +Glc	U	
12	10.06	[M+H] ⁺	C ₁₇ H ₁₄ O ₄	283.098	3.5	255.0646,199.0758,137.0233	Formononetin+CH ₂	U	U
13	10.51	[M+H] ⁺	C ₁₆ H ₁₄ O ₄	271.0959	-4.1	256.0719,163.0394,137.0604	Formononetin+H ₂	P.U	U
14	10.52	[M+H] ⁺	C ₁₇ H ₁₄ O ₅	299.0913	-2.0	284.0680,256.0719,227.0686	Formononetin+O+CH ₂	U	U
15	10.72	[M+H] ⁺	C ₁₇ H ₁₄ O ₅	299.0933	4.7	269.0807,253.0493,237.0543,197.0604	Formononetin+O+CH ₂ isomer	P.U	U
16	11.72	[M+H] ⁺	C ₁₇ H ₁₄ O ₄	283.0969	-0.4	255.0646,199.0758,137.0233	Formononetin+CH ₂	P.U.F	
17	11.12	[M+Na] ⁺	C ₄₁ H ₆₈ O ₁₄	807.4514	0.9	605.4057,587.3896,473.3635,455.3527, 437.3425,419.3323,143.1075	Astragalosides IV	P.U.F	P.U.F
18	9.63	[M+H] ⁺	C ₄₇ H ₇₈ O ₁₉	947.5219	0.3	473.3648,455.3553,437.3402,419.3300	Astragalosides IV+glc	F	F

19	9.95	[M+H] ⁺	C ₄₇ H ₇₈ O ₁₉	947.5189	-3.6	473.3606,455.3512,437.3408,419.3302, 143.1073	Astragalosides IV+glc isomer	U	U
20	10.13	[M+H] ⁺	C ₄₇ H ₇₈ O ₁₉	947.5204	-1.3	473.3644,455.3531,437.3418,419.3310	Astragalosides IV+glc isomer	F	U
21	10.24	[M+H] ⁺	C ₄₆ H ₇₆ O ₁₈	917.5084	-2.8	473.3623,455.3541,437.3409,419.3323, 143.1066	Astragalosides IV+rha	F	
22	10.37	[M+H] ⁺	C ₄₇ H ₇₈ O ₁₉	947.521	-0.6	473.3605,455.3522,437.3414,419.3304, 143.1079	Astragalosides IV+glc isomer	U.F	
23	10.85	[M+H] ⁺	C ₄₇ H ₇₈ O ₁₉	947.5199	-1.8	473.3643,455.3500,437.3401,419.3310, 143.1068	Astragalosides IV+glc isomer	U.F	U
24	10.99	[M+H] ⁺	C ₄₁ H ₆₆ O ₁₄	783.4533	0.3	471.3516,453.3370,435.3259,417.3163, 143.1066	Astragalosides IV-H ₂	F	F
25	10.99	[M+H] ⁺	C ₄₁ H ₆₄ O ₁₃	765.4416	-1.2	473.3602,455.3522,437.3414	Astragalosides IV-H ₂ O	F	F
26	11.5	[M+H] ⁺	C ₄₇ H ₇₆ O ₁₈	929.5094	-1.0	473.3610,455.3524,437.3404	Astragalosides IV+glc-H ₂ O	F	
27	11.99	[M+Na] ⁺	C ₃₆ H ₆₀ O ₁₀	675.4064	-3.0	473.3634,455.3514,437.3405,419.3290	Astragalosides IV-rha	U.F	U.F
28	11.99	[M+Na] ⁺	C ₃₅ H ₅₈ O ₉	645.3947	-3.2	473.3634,455.3514,437.3405,419.3290	Astragalosides IV-glc	P.U.F	
29	13.61	[M+Na] ⁺	C ₃₀ H ₅₀ O ₅	513.5349	-1.8	473.3618,455.3516,437.3406,419.3306, 143.1075	Astragalosides IV-glc-rha	P.F	F
30	7.96	[M+Na] ⁺	C ₄₂ H ₇₂ O ₁₄	823.479	-3.6	621.4376,441.3721,423.3625,405.3520	Ginsenoside Rg1	P.U.F	P.U.F
31	4.74	[M+Na] ⁺	C ₄₂ H ₇₄ O ₁₆	857.4889	1.6	457.3680,439.3582,421.3451,403.3327	Ginsenoside Rg1+2O+H ₂	U.F	
32	5.65	[M+Na] ⁺	C ₄₂ H ₇₂ O ₁₅	839.4763	-0.7	637.4312,619.4211,439.3546,421.3445, 403.3351	Ginsenoside Rg1+O	F	
33	5.74	[M+Na] ⁺	C ₄₂ H ₇₂ O ₁₅	839.478	1.3	637.4312,619.4211,439.3565,421.3459, 403.3356	Ginsenoside Rg1+O isomer	F	
34	5.78	[M+Na] ⁺	C ₄₂ H ₇₄ O ₁₅	841.4918	-0.8	441.3725,423.3610,405.3484	Ginsenoside Rg1+O+H ₂	U.F	
35	5.99	[M+Na] ⁺	C ₄₂ H ₇₂ O ₁₆	855.4738	2.3	653.4280,635.4173,455.3511,437.3402,	Ginsenoside Rg1+2O	F	

							419.3297,403.3189		
36	6.26	[M+H] ⁺	C ₃₆ H ₆₄ O ₁₁	673.452	-1.0	457.3671,439.3568,421.3464,403.3354	Ginsenoside Rg1+2O+H ₂ -glc	F	
37	6.52	[M+Na] ⁺	C ₄₂ H ₇₀ O ₁₅	837.4589	-2.7	455.3511,437.3402,419.3297,403.3189	Ginsenoside Rg1+O-H ₂	F	
38	6.59	[M+H] ⁺	C ₃₆ H ₆₄ O ₁₁	673.452	-1.0	457.3671,439.3568,421.3464,403.3354	Ginsenoside Rg1+2O+H ₂ -glc isomer	F	
39	7.01	[M+H] ⁺	C ₄₈ H ₈₂ O ₁₉	963.551	-2.0	783.4910,765.4763,603.4276,441.3722, 423.3614,405.3494	Ginsenoside Rg1+glc	F	F
40	7.01	[M+H] ⁺	C ₅₂ H ₈₈ O ₂₂	1065.5879	3.2	885.5212,735.4732,585.4171441.3722, 423.3614,405.3494	Ginsenoside Rg1+2rha	F	
41	7.15	[M+H] ⁺	C ₄₈ H ₈₂ O ₁₉	963.5558	3.0	783.4941,765.4805,603.4276,441.3732, 423.3622,405.3521	Ginsenoside Rg1+glc	U.F	
42	7.34	[M+H] ⁺	C ₅₄ H ₉₂ O ₂₄	1125.6099	3.7	945.5400,765.4802,639.4477,621.4366, 441.3727,423.3618,405.3513	Ginsenoside Rg1+2glc	F	
43	7.41	[M+H] ⁺	C ₄₈ H ₈₂ O ₁₉	963.5511	0.3	783.4922,765.4791,603.4252,441.3718, 423.3615,405.3509	Ginsenoside Rg1+glc isomer	U.F	
44	7.46	[M+H] ⁺	C ₄₇ H ₈₀ O ₁₈	933.5433	1.1	753.4789,603.4252,441.3718,423.3615, 405.3509	Ginsenoside Rg1+rha	F	
45	7.56	[M+H] ⁺	C ₄₈ H ₈₂ O ₁₉	963.5511	-1.9	783.4890,765.47761,603.4238,441.3713, 423.3609,405.3495	Ginsenoside Rg1+glc	U.F	
46	7.64	[M+H] ⁺	C ₄₇ H ₈₀ O ₁₈	933.5443	2.1	753.4826,603.4263,441.3720,423.3616, 405.3508	Ginsenoside Rg1+rha isomer	U.F	
47	8.93	[M+Na] ⁺	C ₄₄ H ₇₄ O ₁₅	865.4923	-0.2	801.4631,639.4470,441.3731,423.3618, 405.3504	Ginsenoside Rg1+C ₂ H ₂ O	F	
48	9.45	[M+Na] ⁺	C ₄₄ H ₇₄ O ₁₅	865.4967	4.9	801.4631,639.4470,441.3719,423.3612, 405.3506	Ginsenoside Rg1+C ₂ H ₂ O isomer	F	

49	10.56	[M+Na] ⁺	C ₃₆ H ₆₂ O ₉	661.4369	-3.5	621.4370,603.4264,441.3718,423.3615, 405.3507	Ginsenoside Rg1-glc	U.F	U
50	11.27	[M+Na] ⁺	C ₃₆ H ₆₂ O ₉	661.4413	2.3	621.4367,603.4257,441.3725,423.3617, 405.3511	Ginsenoside Rg1-glc isomer	U.F	F
51	11.93	[M+H] ⁺	C ₃₆ H ₆₀ O ₉	637.4343	4.2	619.4246,457.3673,439.3569,421.3461	Ginsenoside Rg1-glc-H ₂	U.F	
52	13.32	[M+H] ⁺	C ₃₆ H ₆₀ O ₈	621.4377	1.8	603.4276,441.3736,423.3628,405.3521	Ginsenoside Rg1-glc-H ₂ O	U.F	F
53	13.58	[M+H] ⁺	C ₃₆ H ₆₀ O ₈	621.437	0.6	603.4263,441.3724,423.3616,405.3508	Ginsenoside Rg1-glc-H ₂ O isomer	U.F	U.F
54	14.46	[M+H] ⁺	C ₃₀ H ₅₂ O ₄	477.3943	-0.2	459.3846,441.3730,423.3622,405.3517	Protopanaxatriol	P.F	F
55	10.26	[M+Na] ⁺	C ₅₄ H ₉₂ O ₂₃	1131.592	0.2	749.4827,605.44198,443.3881,425.3780, 407.3672	Ginsenoside Rb1	P.U.F	P.U.F
56	8.34	[M+Na] ⁺	C ₅₄ H ₉₂ O ₂₄	1147.5907	2.7	1107.5994,765.4803,603.4290,441.3748, 423.3615,405.3507	Ginsenoside Rb1+O	U.F	
57	9.58	[M+H] ⁺	C ₆₀ H ₁₀₂ O ₂₈	1271.6665	2.3	1091.6078,929.5482,749.4762,605.4431, 443.3884,425.3786,407.3672	Ginsenoside Rb1+glc	U.F	
58	11.38	[M+Na] ⁺	C ₄₈ H ₈₂ O ₁₈	969.5385	-1.4	767.4957,587.4269,443.3879,425.3781, 407.3665	Ginsenoside Rd	U.F	F
59	11.83	[M+Na] ⁺	C ₄₈ H ₈₂ O ₁₈	969.5431	3.3	767.4941,587.4319,443.3877,425.3762, 407.3680	Ginsenoside Rd isomer	U.F	
60	12.53	[M+H] ⁺	C ₃₆ H ₆₂ O ₉	639.4455	-2.7	441.3723,423.3616,405.3520	Ginsenoside Rb1-3glc+O	F	
61	12.68	[M+H] ⁺	C ₃₆ H ₆₂ O ₉	639.4472	0.1	441.3730,423.3620,405.3522	Ginsenoside Rb1-3glc+O isomer	F	
62	12.87	[M+H] ⁺	C ₃₆ H ₆₂ O ₉	639.4501	4.5	441.3723,423.3622,405.3543	Ginsenoside Rb1-3glc+O isomer	F	
63	13.06	[M+H] ⁺	C ₃₆ H ₆₂ O ₁₀	655.4426	0.8	441.3719,423.3610,405.3515	Ginsenoside Rb1-3glc+2O	F	
64	13.32	[M+H] ⁺	C ₄₂ H ₇₂ O ₁₃	785.5064	1.7	605.4420,443.3886,425.3772,407.3663	GinsenosideF2 isomer	U.F	F
65	14.13	[M+H] ⁺	C ₄₂ H ₇₂ O ₁₃	785.5076	3.2	605.4421,443.3889,425.3784,407.3679	GinsenosideF2	U.F	F
66	14.32	[M+H] ⁺	C ₄₂ H ₇₂ O ₁₃	785.5052	0.1	605.4439,443.3882,425.3778,407.3667	Ginsenoside20(S)Rg3	F	F

67	16.24	[M+H] ⁺	C ₃₆ H ₆₂ O ₈	623.4543	3.2	443.3886,425.3780,407.3679	Ginsenoside Rb1-3glc	F	F
68	16.45	[M+H] ⁺	C ₃₆ H ₆₂ O ₈	623.459	4.7	443.3877,425.3780,407.3661	Ginsenoside Rb1-3glc isomer	F	F
69	16.45	[M+H] ⁺	C ₃₀ H ₅₂ O ₄	477.3951	1.5	441.3721,423.3628,405.3526	Ginsenoside Rb1-4glc+O	F	
70	19.95	[M+H] ⁺	C ₃₀ H ₅₂ O ₃	461.4012	3.7	443.3881,425.3777,407.3674	Protopanaxadiol	P.U.F	P.U.F
71	7.47	[M-H] ⁻	C ₃₆ H ₃₀ O ₁₆	717.145	-0.8	519.0920,339.0510,321.0406,295.0603, 293.0445	Salvianolic acid B	F	F
72	2.63	[M-H] ⁻	C ₉ H ₉ NAO ₅	219.028	5.0	197.0443,179.0341	Sodium Danshensu	F	
73	4.66	[M-H] ⁻	C ₁₈ H ₁₈ O ₈	361.0938	4.2	317.1034,273.1132,257.0827,239.0575, 221.0472,195.0666,177.0579	Salvianolic acid R	F	F
74	6.02	[M-H] ⁻	C ₂₇ H ₂₄ O ₁₂	539.1185	-0.9	495.1293,359.0746,315.0890,297.0761, 255.0796	Salvianolic acid S	F	
75	6.27	[M-H] ⁻	C ₂₇ H ₂₄ O ₁₂	539.1186	-0.7	495.1272,399.0716,315.0876,297.0764, 255.0797	Salvianolic acid S isomer	F	F
76	7.06	[M-H] ⁻	C ₂₇ H ₂₂ O ₁₂	537.1047	2.6	339.0500,321.0435,295.0618,255.0789	Lithospermic acid A	F	
77	8.05	[M-H] ⁻	C ₃₇ H ₃₂ O ₁₆	731.1596	-2.2	533.1100,353.0604,339.0509,335.0555, 321.0399	Salvianolic acid B+CH ₂	F	
78	8.58	[M-H] ⁻	C ₃₇ H ₃₂ O ₁₆	731.1624	1.6	533.1077,353.0663,339.0506,335.0551, 321.0409	Salvianolic acid B+CH ₂ isomer	F	
79	8.79	[M-H] ⁻	C ₃₇ H ₃₂ O ₁₆	731.1612	0.1	533.1085,353.0699,339.0501,335.0546, 321.0385	Salvianolic acid B+CH ₂ isomer	F	
80	8.86	[M-H] ⁻	C ₃₈ H ₃₄ O ₁₆	745.1747	-3.0	533.1090,353.0667,335.0557,309.0771, 307.0605	Salvianolic acid B+2CH ₂	F	
81	9.15	[M-H] ⁻	C ₃₈ H ₃₄ O ₁₆	745.1772	0.4	547.1234,339.0547,321.0423,295.0601, 293.0485	Salvianolic acid B+2CH ₂ isomer	F	

82	9.45	[M-H] ⁻	C ₃₉ H ₃₆ O ₁₆	759.1929	0.5	547.1216,353.0657,335.0563,321.0399	Salvianolic acid B+3CH ₂	F		
83	9.47	[M-H] ⁻	C ₃₈ H ₃₄ O ₁₆	745.1777	1.1	547.1230,353.0680,335.0514	Salvianolic acid B+2CH ₂ isomer	F		
84	17.49	[M+Na] ⁺	C ₁₉ H ₁₈ O ₃	317.115	-1.3	277.1216,262.0982,249.1277,234.1037, 231.1171,221.1335,206.1082,191.0851	Tanshinone IIA	P.U.F	U.F	
85	9.98	[M+Na] ⁺	C ₁₉ H ₂₀ O ₅	351.1199	-2.6	311.1253,267.1381,225.0908	Tanshinone IIA+2O+H ₂	P.U		
86	10.72	[M+Na] ⁺	C ₁₉ H ₁₈ O ₅	349.105	-0.6	309.1126,265.1214,223.0733	Tanshinone IIA+2O	U.F		
87	11.70	[M+Na] ⁺	C ₁₉ H ₁₆ O ₄	349.105	-0.6	309.1123,265.1234,223.0726	Tanshinone IIA+2O isomer	P.U		
88	11.86	[M+Na] ⁺	C ₁₉ H ₁₆ O ₄	349.105	-0.6	309.1098,265.1237,223.0762	Tanshinone IIA+2O isomer	U.F		
89	12.17	[M+Na] ⁺	C ₁₉ H ₁₈ O ₄	333.1096	-2.1	293.1164,275.1079	Tanshinone IIB	P.U	U	
90	12.34	[M+Na] ⁺	C ₁₉ H ₂₀ O ₅	351.1203	-1.4	311.1283,267.1378,225.0893	Tanshinone IIA+2O+H ₂ isomer	P.U.F	U	
91	12.57	[M+Na] ⁺	C ₁₉ H ₂₀ O ₅	351.1203	-1.4	311.1275,283.1319,267.1369	Tanshinone IIA+2O+H ₂ isomer	P		
92	12.99	[M+Na] ⁺	C ₁₉ H ₁₈ O ₅	349.105	-0.6	309.1106,265.1222,223.0723	Tanshinone IIA+2O isomer	P.U.F		
93	13.58	[M+Na] ⁺	C ₁₉ H ₁₈ O ₄	333.1094	-2.7	293.1169,247.1143	Tanshinone IIA+O	P.F		
94	13.92	[M+Na] ⁺	C ₁₉ H ₂₀ O ₅	351.1209	0.3	311.1263,283.1324,267.1364	Tanshinone IIA+2O+H ₂ isomer	P.U.F		
95	13.98	[M+Na] ⁺	C ₁₉ H ₁₈ O ₄	333.1095	-2.4	283.1337,281.0809,265.1227	Tanshinone IIA+O isomer	P.F		
96	14.09	[M+Na] ⁺	C ₁₉ H ₂₀ O ₄	335.1248	-3.3	295.1329,267.1380,252.1142,237.0919	Tanshinone IIA+O+H ₂	P.U.F		
97	14.68	[M+Na] ⁺	C ₁₉ H ₂₂ O ₄	337.1405	-3.3	297.1485,279.1380,268.1083,251.1440	Tanshinone IIA+O+2H ₂	P.U.F	P.U	
98	14.81	[M+Na] ⁺	C ₂₀ H ₂₂ O ₅	365.1349	-4.4	325.1423,311.1264,265.1207,251.1053	Tanshinone IIA+2O+CH ₂	U.F		
99	14.93	[M+Na] ⁺	C ₂₀ H ₂₂ O ₅	365.1351	-3.8	325.1423,311.1266,269.1168,267.1373, 251.1055	Tanshinone IIA+2O+CH ₂	F		
100	15.79	[M+Na] ⁺	C ₂₀ H ₂₀ O ₄	347.1248	-3.2	293.1165,275.1069,247.1114,219.1166	Tanshinone IIA+O+CH ₂	F		
101	16.65	[M+Na] ⁺	C ₁₉ H ₁₆ O ₃	315.1001	1.3	275.1064,247.1107,219.1158	Tanshinone IIA-H ₂	F		

102	7.66	[M+H] ⁺	C ₃₁ H ₄₃ NO ₁₀	590.2969	0.7	572.2847,558.2696,540.2590,526.2435, 508.2324,494.2162,482.2169,476.2064	Benzoylmesaconine	P.U	U.F
103	3.81	[M+H] ⁺	C ₂₄ H ₃₉ NO ₉	486.2687	-3.3	454.2419,436.2308,404.2026	Mesaconine*	P.U.F	P.U.F
104	4.78	[M+H] ⁺	C ₂₄ H ₃₉ NO ₈	470.275	-0.9	438.2404	Hypaconine*	U	P.U.F
105	6.23	[M+H] ⁺	C ₃₀ H ₄₁ NO ₁₀	576.28	-1.6	558.2648,526.2432,512.2304,494.2162	Benzoylmesaconine-CH ₂	F	
106	6.33	[M+H] ⁺	C ₃₀ H ₄₁ NO ₁₀	576.2786	-4.0	558.2686,526.2441,512.2224,494.2113	Benzoylmesaconine-CH ₂ isomer	U.F	
107	6.46	[M+H] ⁺	C ₃₁ H ₄₃ NO ₁₁	606.291	-0.7	588.2772,574.2632,556.2540,524.2277	Benzoylmesaconine+O	F	
108	6.58	[M+H] ⁺	C ₃₁ H ₄₃ NO ₁₁	606.2927	2.1	588.2809,574.2679,556.2513,524.2244	Benzoylmesaconine+O isomer	F	
109	6.64	[M+H] ⁺	C ₃₁ H ₄₃ NO ₁₁	606.2932	3.0	588.2808,574.2650,556.2537,524.2278	Benzoylmesaconine+O isomer	F	U.F
110	6.82	[M+H] ⁺	C ₃₂ H ₄₅ NO ₁₁	620.3058	-2.1	588.2816,570.2746,556.2548	Benzoylmesaconine+O+CH ₂	F	
111	6.89	[M+H] ⁺	C ₃₂ H ₄₅ NO ₁₀	604.2778	2.0	576.2819,554.2758,540.2593	Benzoylmesaconine+CH ₂	F	
112	7.13	[M+H] ⁺	C ₃₀ H ₄₁ NO ₁₀	576.2803	-1.0	558.2621,526.2411,512.2236,494.2171	Benzoylmesaconine-CH ₂ isomer	U	F
113	7.23	[M+H] ⁺	C ₃₁ H ₄₁ NO ₁₀	588.2814	0.8	570.2694,556.2525	Benzoylmesaconine-H ₂	U	
114	7.52	[M+H] ⁺	C ₃₁ H ₄₃ NO ₉	574.3013	-0.5	556.2959,542.2712,524.2652,510.2460	Benzoylmesaconine-H ₂ O+H ₂	U	
115	7.63	[M+H] ⁺	C ₃₀ H ₄₁ NO ₁₀	576.2805	-0.7	558.2621,526.2411,512.2236,494.2171	Benzoylmesaconine-CH ₂ isomer	U	
116	8.06	[M+H] ⁺	C ₃₁ H ₄₃ NO ₉	574.3013	-0.5	556.2959,542.2712,524.2652,510.2460 isomer	Benzoylmesaconine-H ₂ O+H ₂ isomer	U	
117	8.19	[M+H] ⁺	C ₃₁ H ₄₃ NO ₉	574.3013	-0.5	556.2908,542.2755,524.2651,510.2452	Benzoylmesaconine-H ₂ O+H ₂ isomer	U	U
118	8.23	[M+H] ⁺	C ₃₂ H ₄₅ NO ₁₀	604.3118	-0.7	576.2812,554.2698,540.2574	Benzoylmesaconine+CH ₂ isomer	U	U
119	9.76	[M+H] ⁺	C ₃₂ H ₄₃ NO ₁₀	602.2949	-2.7	584.2823,542.2754,510.2492	Benzoylmesaconine-H ₂ +CH ₂	U	
120	8.81	[M+Na] ⁺	C ₃₆ H ₅₆ O ₁₃	719.3614	-0.7	535.3294,391.2472,373.2356,355.2261, 337.2150	Periplocin	U.F	F
121	4.33	[M+Na] ⁺	C ₂₃ H ₃₆ O ₆	431.2401	-2.1	391.2475,373.2357,355.2269,337.2162	Periplogenin+H ₂ +O	F	
122	5.91	[M+H] ⁺	C ₂₃ H ₃₄ O ₆	407.2432	-0.5	389.2326,371.2223,353.2114,335.2009	Periplogenin+O	F	

123	6.22	[M+Na] ⁺	C ₂₃ H ₃₆ O ₆	431.239	-4.6	391.2443,373.2372,355.2259,337.2150	Periplogenin+H ₂ +O isomer	F	
124	6.94	[M+H] ⁺	C ₂₃ H ₃₄ O ₅	391.2476	-2.0	373.2372,355.2264,337.2153	Periplogenin isomer	F	
125	7.22	[M+H] ⁺	C ₂₃ H ₃₄ O ₆	407.2432	-0.5	389.2326,371.2223,353.2114,335.2009	Periplogenin+O isomer	F	
126	7.61	[M+Na] ⁺	C ₂₃ H ₃₆ O ₆	431.239	-4.6	391.2509,373.2372,355.2268,337.2167	Periplogenin+H ₂ +O isomer	P.U.F	
127	8.87	[M+H] ⁺	C ₃₂ H ₅₀ O ₁₀	595.3506	4.0	535.3256,517.3168,373.2356,355.2261, 337.2150	Periplocyamarin+H ₂ +O	F	F
128	9.22	[M+H] ⁺	C ₂₃ H ₃₄ O ₅	391.2476	-2.0	373.2372,355.2264,337.2153	Periplogenin	P.U	P.U
129	9.41	[M+Na] ⁺	C ₂₉ H ₄₆ O ₉	561.3065	4.5	391.2468,373.2365,355.2261,337.2168	Periplocyamarin-CH ₂ +H ₂ +O	P.U.F	
130	9.55	[M+H] ⁺	C ₃₀ H ₄₈ O ₈	537.3422	-0.9	375.2528,357.2428,339.2316	Periplocyamarin+H ₂	P.U.F	
131	9.86	[M+H] ⁺	C ₂₉ H ₄₄ O ₈	521.3124	1.9	391.2470,373.2375,355.2264,337.2166	Periplocyamarin-CH ₂	P.U.F	
132	10.16	[M+H] ⁺	C ₂₉ H ₄₆ O ₈	523.3282	2.1	505.3180,487.3104,375.2533,357.2432, 339.2321	Periplocyamarin-CH ₂ +H ₂	P.U.F	
133	10.88	[M+H] ⁺	C ₃₀ H ₄₆ O ₈	535.3264	-1.3	499.3043,391.2473,373.2366,355.2264, 337.2154	Periplocyamarin	P.U.F	F
134	11.15	[M+H] ⁺	C ₃₀ H ₄₈ O ₈	537.3425	-0.4	375.2528,357.2428,339.2316	Periplocyamarin+H ₂ isomer	P.U.F	
135	15.42	[M+Na] ⁺	C ₃₀ H ₅₀ O ₅	513.3536	-3.9	473.3619,455.3523,437.3418,383.2938, 365.2836,339.2684	Alisol A	P.U.F	P.U.F
136	9.56	[M+H] ⁺	C ₃₀ H ₄₈ O ₈	537.3439	2.2	519.3318,501.3211,483.3109,465.3011, 447.2873	Alisol A+3O-H ₂	F	
137	10.09	[M+H] ⁺	C ₂₉ H ₄₆ O ₆	491.3375	0.4	473.3276,455.3172,437.3047,419.2917, 401.2694	Alisol A-CH ₄ +O	F	
138	10.34	[M+H] ⁺	C ₂₉ H ₄₆ O ₆	491.3369	-0.8	473.3270,455.3146,437.3045,419.2924, 401.2694	Alisol A-CH ₄ +O isomer	F	F
139	10.37	[M+H] ⁺	C ₂₉ H ₄₄ O ₆	489.3211	-1.0	471.3102,453.3003,435.2904	Alisol A-CH ₄ +O-H ₂	F	
140	10.62	[M+H] ⁺	C ₂₉ H ₄₄ O ₆	489.3214	-0.4	471.3102,453.3003,435.2904	Alisol A-CH ₄ +O-H ₂ isomer	F	

141	10.94	[M+H] ⁺	C ₃₀ H ₄₈ O ₇	521.3472	-1.2	503.3374,485.3268,467.3157,449.3055	Alisol A+2O-H ₂	P.U.F	
142	11.05	[M+H] ⁺	C ₃₀ H ₄₈ O ₆	505.353	0.2	487.3336,469.3363	Alisol A+O-H ₂	U.F	P.U.F
143	11.36	[M+H] ⁺	C ₃₀ H ₄₆ O ₇	519.3319	-0.6	501.3211,483.3109,465.3011,447.2873	Alisol A+2O-2H ₂	P.F	
144	11.84	[M+Na] ⁺	C ₂₉ H ₄₆ O ₇	529.3127	-2.6	489.3216,471.3111,453.3000,435.2896	Alisol A-CH ₄ +2O	F	
145	11.99	[M+H] ⁺	C ₃₀ H ₅₀ O ₇	523.3638	0.6	505.3505,487.3346,469.3365	Alisol A+2O	P.U	
146	12.09	[M+H] ⁺	C ₃₀ H ₅₀ O ₆	507.3667	-3.7	489.3580,471.3498,453.3358,381.2779, 363.2683	Alisol A+O	P.U.F	P.U.F
147	12.48	[M+Na] ⁺	C ₃₆ H ₅₆ O ₁₁	687.3744	3.5	647.3800,471.3479,453.3384,435.3279, 413.3073,395.2952	Alisol A-H ₂ +gluA	F	
148	12.66	[M+H] ⁺	C ₃₀ H ₄₆ O ₇	519.3319	-0.6	501.3211,483.3109,465.3011,447.2873	Alisol A+2O-2H ₂ isomer	P.F	
149	12.7	[M+H] ⁺	C ₃₀ H ₄₈ O ₇	521.3472	-1.2	503.3374,485.3268,467.3157,449.3055	Alisol A+2O-H ₂ isomer	P.U.F	P.U.F
150	12.91	[M+H] ⁺	C ₃₆ H ₅₆ O ₁₀	649.3959	1.1	473.3601,455.3578,437.3510,383.3021, 365.2843,339.2707	Alisol A-H ₂ O+gluA	F	
151	12.99	[M+Na] ⁺	C ₃₆ H ₅₈ O ₁₁	689.3865	-1.7	473.3606,455.3503,437.3510,383.2939, 365.2858,339.2675	Alisol A+gluA	P.U	P.F
152	13.13	[M+H] ⁺	C ₃₀ H ₄₆ O ₇	519.3337	2.9	501.3211,483.3109,465.3011,447.2873	Alisol A+2O-2H ₂ isomer	P.F	P.F
153	13.51	[M+Na] ⁺	C ₃₆ H ₅₈ O ₁₁	689.3843	-4.9	473.3621,455.3523,437.3403,383.2937, 365.2841,339.2672	Alisol A+gluA isomer	F	
154	13.66	[M+Na] ⁺	C ₃₆ H ₅₆ O ₁₁	687.3744	3.5	647.3800,471.3479,453.3384,435.3279, 413.3073,395.2952	Alisol A-H ₂ + gluA isomer	F	
155	14.11	[M+Na] ⁺	C ₃₀ H ₄₈ O ₅	511.3399	0.1	471.3456,453.3301,381.2784,337.2509	Alisol A-H ₂	P.F	P
156	4.77	[M-SCN] ⁺	C ₁₆ H ₂₄ NO ₅	310.1649	-1.4	251.0908,207.0648,175.0389,147.0441, 119.0492	Sinapine thiocyanate	U	U
157	5.65	[M+H] ⁺	C ₁₁ H ₁₄ O ₅	227.0923	1.8	209.0818,167.0712	Sinapine thiocyanate-C ₅ H ₁₂ N ⁺ +H ₂	U.F	

158	5.88	[M+H] ⁺	C ₁₁ H ₁₂ O ₅	225.0776	0.2	207.0648,167.0709	Sinapine thiocyanate-C ₅ H ₁₂ N ⁺	U.F	U
159	6.27	[M+H] ⁺	C ₁₁ H ₁₂ O ₅	225.0776	0.2	207.0648,181.0876	Sinapine thiocyanate-C ₅ H ₁₂ N ⁺	U	U
160	8.77	[M+H] ⁺	C ₁₂ H ₁₄ O ₅	239.091	-3.8	207.0648	Sinapine thiocyanate-C ₄ H ₁₀ N ⁺	U.F	U.F
161	6.79	[M-H] ⁻	C ₂₇ H ₃₂ O ₁₄	579.1721	1.0	459.1160,271.0613,151.0043	Naringin	P.U.F	U.F
162	5.43	[M-H] ⁻	C ₁₅ H ₁₂ O ₈ S	351.0183	2.3	271.0614,151.0039,119.0502	Naringenin+sul	U	
163	5.92	[M-H] ⁻	C ₂₁ H ₂₀ O ₁₄ S	527.0472	-4.6	351.0177,271.0600,151.0044	Naringenin+sul+gluA	P	
164	6.53	[M-H] ⁻	C ₁₅ H ₁₀ O ₈ S	349.0015	-0.9	269.0461,117.0348	Apigenin+sul	P	
165	6.89	[M-H] ⁻	C ₂₁ H ₂₀ O ₁₁	447.0941	3.1	271.0613,151.0058	Naringenin+gluA	P	
166	7.22	[M-H] ⁻	C ₂₈ H ₃₄ O ₁₅	609.1824	0.8	301.0717,271.0658,151.0043	Hesperidin	F	
167	7.52	[M-H] ⁻	C ₁₅ H ₁₂ O ₈ S	351.0186	3.1	271.0612,151.0042,119.0506	Naringenin+sul isomer	U	
168	7.54	[M-H] ⁻	C ₂₁ H ₂₀ O ₁₁	447.0931	0.9	271.0621,151.0039	Naringenin+gluA isomer	P	P
169	7.62	[M-H] ⁻	C ₂₇ H ₃₄ O ₁₄	581.188	1.7	273.0763,179.0344,119.0507	Naringin+H ₂	F	
170	7.67	[M-H] ⁻	C ₁₅ H ₁₀ O ₈ S	349.0028	2.9	269.0464,151.0054,119.0491	Apigenin+sul isomer	F	
171	7.69	[M-H] ⁻	C ₁₅ H ₁₂ O ₈ S	351.017	-1.4	271.0625,151.0010,119.0457	Naringenin+sul isomer	P	
172	7.88	[M-H] ⁻	C ₁₆ H ₁₄ O ₆	381.0284	1.0	301.0717,151.0026	Hesperetin+sul	U	
173	9.05	[M-H] ⁻	C ₁₅ H ₁₂ O ₅	271.0616	3.7	177.0198,151.0041,119.0517	Naringenin	P.U.F	
174	9.09	[M-H] ⁻	C ₁₅ H ₁₀ O ₅	269.0458	3.0	151.0041,119.0503	Apigenin	U.F	
175	9.23	[M-H] ⁻	C ₁₅ H ₁₄ O ₅	273.0763	0.1	167.0351	Hydrogenated naringin	F	
176	9.56	[M-H] ⁻	C ₁₆ H ₁₄ O ₆	301.0719	1.6	151.0059	Hesperetin	F	

Note: P: plasma, F: feces, U: urine, B: bile, sul: sulfation, gluA: glucuronidation. *Compounds identified by comparing with reference standards.

Table 2 Characterization of *in vivo* metabolites of QLQX in rats (metabolites characterized in Table 1 are not included).

tR/min	selected ion	elemental composition	Measured	Calculated	ppm	fragmentation	Identification	Source (formula)
			mass	mass				
177	3.23	[M+H] ⁺	C ₂₃ H ₃₇ NO ₆	424.2692	424.2699	-1.5	406.2590,374.2332,356.2235	Isotalatizidine+O U
178	4.32	[M+H] ⁺	C ₂₂ H ₃₁ NO ₃	358.238	358.2383	0.3	340.2262	Songorine P.U
179	4.33	[M+H] ⁺	C ₂₂ H ₃₃ NO ₃	360.2533	360.2539	-0.6	342.2344	Songorine+H ₂ U
180	4.35	[M+H] ⁺	C ₂₃ H ₃₇ NO ₅	408.274	408.2735	-0.5	390.2694,376.2488	Chuanfumine+CH ₂ U
181	4.65	[M+H] ⁺	C ₂₃ H ₃₇ NO ₇	440.2641	440.2648	-0.7	422.2539,390.2303	Fuziline-CH ₂ U
182	4.84	[M+H] ⁺	C ₂₄ H ₃₉ NO ₇	454.2795	454.2791	-0.4	436.2688,404.2414,372.2171	Fuziline P.U
183	4.9	[M+H] ⁺	C ₂₃ H ₃₇ NO ₅	408.274	408.2735	-0.5	390.2694	Karakolidine+CH ₂ U
184	5.09	[M+H] ⁺	C ₂₄ H ₃₉ NO ₆	438.2855	438.286	0.5	420.2757,388.2482,356.2228	Neoline P.U
185	5.12	[M+H] ⁺	C ₂₅ H ₄₁ NO ₇	468.2964	468.2961	0.6	450.2877,418.2403,386.2331	Fuziline+CH ₂ U
186	5.24	[M+H] ⁺	C ₂₄ H ₃₉ NO ₆	438.2842	438.2836	-0.8	420.284,388.2474	Foresticine U
187	5.56	[M+H] ⁺	C ₂₄ H ₃₉ NO ₅	422.2889	422.2877	-1.2	390.2646	Talatizamine P.U
188	5.77	[M+H] ⁺	C ₁₀ H ₈ O ₄	193.0502	193.0509	0.7	178.0272,150.0320,133.0297	Scopoletin U
189	6.07	[M+H] ⁺	C ₂₅ H ₄₁ NO ₆	452.2999	452.2992	-0.7	420.238	Chasmanine P.U
190	6.49	[M+H] ⁺	C ₂₅ H ₃₉ NO ₅	434.291	434.2906	0.4	402.2632	Chasmanine-H ₂ O U
191	6.61	[M+H] ⁺	C ₂₆ H ₄₁ NO ₆	464.3008	464.301	0.2	432.2888,372.2330	14-Acetylitalatisamine U
192	6.71	[M+H] ⁺	C ₂₂ H ₂₀ O ₁₁	461.1084	461.1078	-1.3	285.0831,270.0520,253.0500	Calycosin+gluA P.U
193	6.75	[M+H] ⁺	C ₁₆ H ₁₂ O ₈ S	365.0331	365.0331	0.1	285.0761,270.0511,253.0445	Calycosin+sul U
194	7.83	[M+H] ⁺	C ₂₂ H ₂₀ O ₁₀	445.1104	445.1135	4.6	269.081	Formononetin+guA P

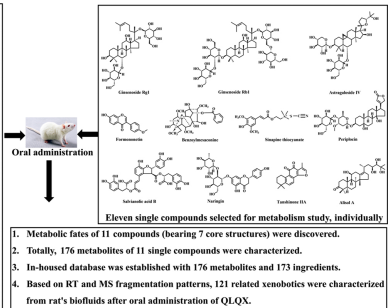
195	8.15	[M+H] ⁺	C ₃₂ H ₄₅ NO ₁₀	604.3127	604.3137	1.7	586.3016,572.2856,554.2750,540.2610,522.2489, 496.2326	Benzoylaconine	U
196	8.49	[M+H] ⁺	C ₃₁ H ₄₃ NO ₈	574.301	574.3009	-0.1	542.2741,510.2477,492.2400	Benzoylhyaconine	U.F
197	8.89	[M+H] ⁺	C ₃₁ H ₄₃ NO ₈	558.3063	558.3065	0.3	526.2752,508.2584,476.2411	14-benzoyl-13-deoxyhyaconine	U
198	9.26	[M+H] ⁺	C ₁₈ H ₂₀ O ₅	317.1399	317.1389	3.2	299.1279,271.1324,253.1225	Neocryptotanshinone-CH ₂ +O	U
199	9.9	[M+H] ⁺	C ₁₉ H ₂₀ O ₄	313.1435	313.144	-1.6	295.1345,267.1385	Cryptotanshione+O	U
200	9.99	[M+Na] ⁺	C ₄₂ H ₇₂ O ₁₄	823.4808	823.4801	-0.7	621.4358,603.4254,441.3744,423.3617,405.3497	Ginsenoside Rf	U
201	10.06	[M+H] ⁺	C ₂₁ H ₂₂ O ₉	419.13452	419.1342	2.4	404.1104,389.389.0878,374.0628,359.0409	Nobiletin+O	U
202	10.26	[M+H] ⁺	C ₁₉ H ₁₈ O ₇	359.113	359.1131	-0.3	344.0888,329.0660,314.0421	Tangeretin-CH ₂	U
203	10.29	[M+H] ⁺	C ₃₃ H ₄₅ NO ₁₀	616.3121	616.3125	0.71	556.2903,524.2631	Hypaconitine	U
204	10.51	[M+H] ⁺	C ₂₀ H ₂₀ O ₈	389.1233	389.1236	-0.8	374.0999,359.0769,344.0531	Nobiletin-CH ₂	U
205	10.62	[M+Na] ⁺	C ₂₇ H ₄₄ O ₆	487.3021	487.3012	-0.9	281.2249,255.209	Periplocoside N	P
206	10.75	[M+H] ⁺	C ₁₇ H ₁₆ O ₅	301.1076	301.1077	0.1	167.0716	(6aR,11aR)-3-hydroxy-9,10-dime thoxypterocarpan	U
207	10.81	[M+Na] ⁺	C ₃₅ H ₆₀ O ₁₇	775.3727	775.3737	0.1	559.7792,423.3631	Perisesaccharide C	U
208	10.98	[M+H] ⁺	C ₂₁ H ₂₂ O ₉	419.13452	419.1342	2.4	404.1104,389.389.0878,374.0628,359.0409	Nobiletin+O	U
209	11.21	[M+H] ⁺	C ₄₁ H ₆₈ O ₁₄	785.4678	785.4687	1.1	473.3622,455.3515,437.3411,419.3302,143.1075	Isoastragalosides IV	F
210	11.08	[M+H] ⁺	C ₃₀ H ₄₈ O ₆	505.3532	505.3541	0.9	487.3419,469.3316,451.3183,415.2827	16-oxo-Alisol A	P.U
211	11.22	[M+H] ⁺	C ₂₀ H ₂₀ O ₉	405.118	405.1186	-0.6	390.0958,375.0719	Natsudaidain-CH ₂	U
212	11.88	[M+Na] ⁺	C ₁₈ H ₂₀ O ₄	323.1258	323.1259	-0.4	283.1335,265.1230,255.1381	Neocryptotanshinone-CH ₂	U
213	12.04	[M+Na] ⁺	C ₁₈ H ₂₀ O ₄	323.1258	323.1259	-0.4	283.1335,265.1230,255.1381	Neocryptotanshinone-CH ₂	U
214	12.08	[M+H] ⁺	C ₃₀ H ₄₈ O ₆	505.3505	505.3529	-4.7	487.3346,469.3365	Alisol F+O	P.U.F
215	12.09	[M+Na] ⁺	C ₅₆ H ₉₂ O ₂₅	1187.5794	1187.5768	-2.6	985.4957,299.2365,281.2256,203.0907	Glycoside H2	U

216	12.16	[M+H] ⁺	C ₄₈ H ₇₈ O ₁₈	943.5238	943.5261	2.3	441.3719,423.3614	Soyasaponin	F
217	12.44	[M+Na] ⁺	C ₃₀ H ₄₆ O ₇	541.3146	541.3141	0.9	501.3220,483.3119,465.3011,447.2873	Alisol C+2O	P
218	12.67	[M+H] ⁺	C ₅₆ H ₉₂ O ₂₅	1165.597	1165.6	-3.0	1187.5804,1001.4602,819.4380,703.4014,317.2487 ,299.2366,281.2270,261.0282,203.0917	Glycoside H2 isomer	U
219	13.05	[M+H] ⁺	C ₃₀ H ₄₆ O ₅	487.341	487.3402	-0.8	469.3312,451.3198,397.2731	Alisol C	P
220	13.03	[M+Na] ⁺	C ₅₆ H ₉₂ O ₂₄	1171.5864	1171.587	0.6	969.50047,805.3820,687.4066,323.1327,309.1123	Pregnane, β-D-galactopyranoside deriv	U
221	13.07	[M+H] ⁺	C ₁₉ H ₁₆ O ₄	309.1116	309.1127	3.6	265.1234,223.0733	Tanshinone IIA+O-H ₂	U.F
222	13.11	[M+H] ⁺	C ₃₀ H ₄₈ O ₅	489.3555	489.3536	-1.9	471.3515,453.3358,399.2862	16-oxo-11-deoxy-Alisol A	P
223	13.17	[M+Na] ⁺	C ₃₀ H ₄₆ O ₇	541.3144	541.3141	0.6	501.3220,483.3119,465.3011,447.2873	Alisol C+2O	P.U.F
224	13.52	[M+Na] ⁺	C ₁₉ H ₂₂ O ₄	337.1406	337.141	0.4	297.1483,253.1596,223.1103	Neocryptotanshinone	P.U
225	13.88	[M+Na] ⁺	C ₃₀ H ₄₈ O ₇	543.3286	543.3298	-2.2	503.3358,485.3261,467.3074	16-oxo-Alisol A+O	P
226	14.31	[M+Na] ⁺	C ₃₀ H ₄₆ O ₇	541.3144	541.3141	0.6	501.3220,483.3119,465.3011,447.2873	Alisol C+2O	P
227	14.43	[M+Na] ⁺	C ₃₀ H ₅₀ O ₅	513.355	513.3556	-1.2	473.3619,455.3523,437.3418,383.2938,365.2836, 339.2684	11-deoxy-alisol A+O	U.F
228	17.07	[M+Na] ⁺	C ₃₀ H ₆₀ O ₈	643.4178	643.4186	-1.2	441.3721,423.3625,405.3520	Ginsenoside Re-2glc	U
229	17.72	[M+Na] ⁺	C ₃₀ H ₄₄ O ₄	491.3086	491.3118	3.2	451.3201,433.3127,411.2889,397.2732	Alisol L isomer	P
230	17.81	[M+Na] ⁺	C ₃₀ H ₄₆ O ₄	493.328	493.3271	-0.9	453.3377,339.2661	16,23-Oxido-alisol B	P
231	17.87	[M+Na] ⁺	C ₃₀ H ₄₈ O ₄	495.3435	495.3426	-0.9	455.3498,383.2933	Alisol B	P
232	19.19	[M+Na] ⁺	C ₆₅ H ₁₀₆ O ₂₄	1293.6961	1293.6955	-0.6	281.2263,255.2103,203.0914,171.0653	Periplocoside E	P

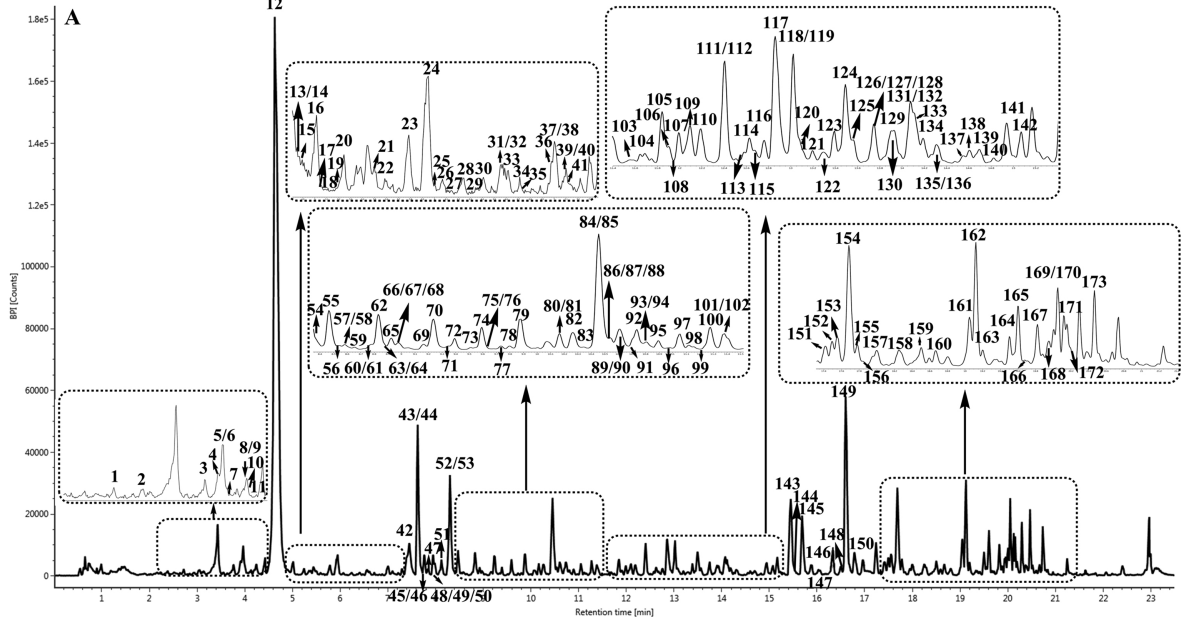
Note: P: plasma, F: feces, U: urine, B: bile, sul: sulfation, gluA: glucuronidation.*Compounds identified by comparing with reference standards.

Highlights

1. Chemical recognition of QLQX was performed, and 173 ingredients were identified.
2. Metabolism of 11 compounds was studied, and 176 metabolites were characterized.
3. Holistic metabolic profiles of multi-ingredients in QLQX were revealed.
4. A total of 121 QLQX-related xenobiotics were characterized in rat's biofluids.



Graphics Abstract



Item name: 2016090808
Channel name: 1: TOF MS¹ BPI (50-2000) 4eV, 0eV ESI:

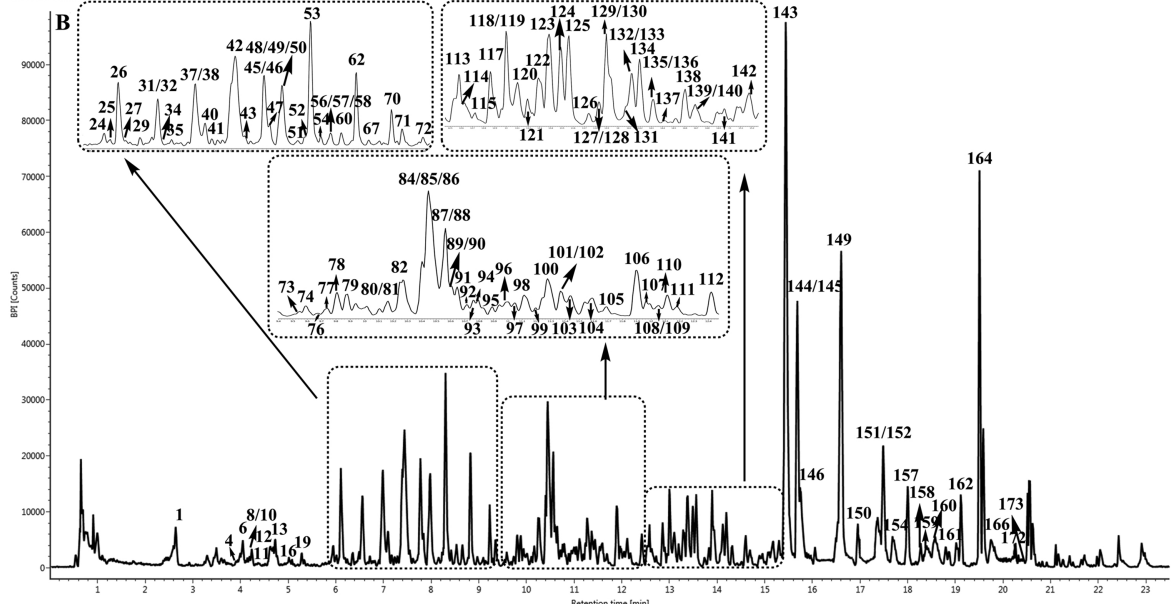


Figure 1

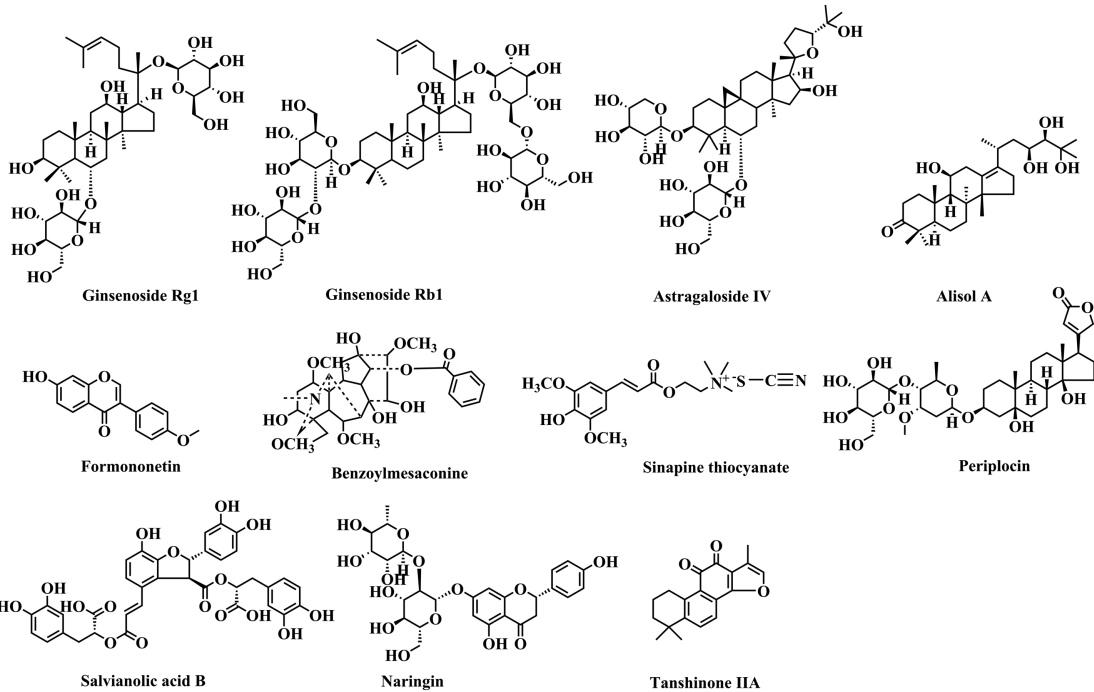


Figure 2

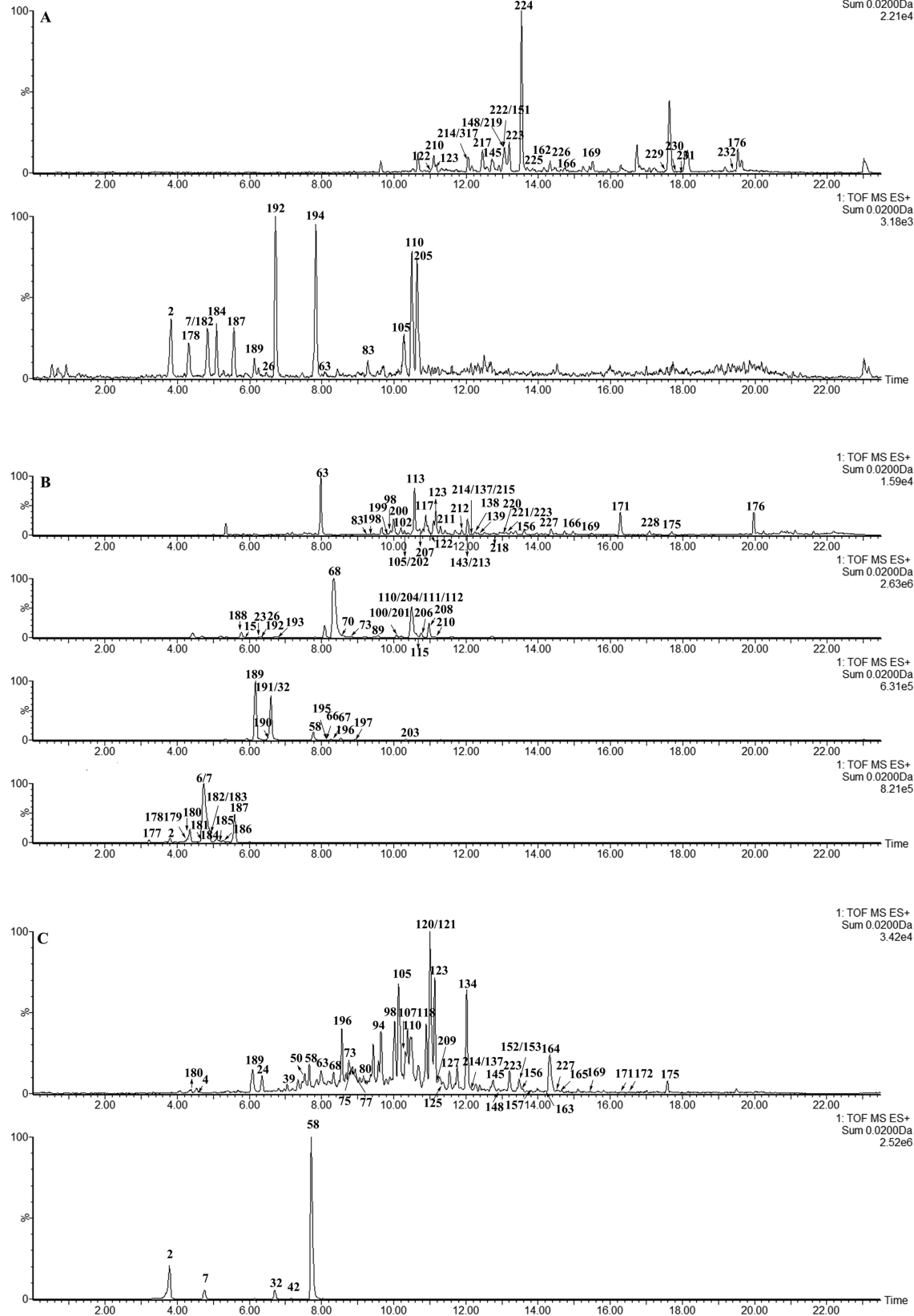


Figure 3